

# Red, Gas Rich Low Surface Brightness Galaxies And Enigmatic Deviations from the Tully-Fisher Relation

K. O'Neil

Arecibo Observatory, HC03 Box 53995, Arecibo, PR 00612

*koneil@naic.edu*

G. D. Bothun

and

J. Schombert

Physics Department, University of Oregon, Eugene, OR 97403

*nuts@bigmoo.uoregon.edu, js@abyss.uoregon.edu*

Received \_\_\_\_\_; accepted \_\_\_\_\_

## ABSTRACT

Using the refurbished 305m Arecibo Gregorian Telescope, we detected 43 low surface brightness (LSB) galaxies from the catalog of O’Neil, Bothun, & Cornell (1997a). The detected galaxies range from  $22.0 \text{ mag arcsec}^{-2} \leq \mu_B(0) \leq 25.0 \text{ mag arcsec}^{-2}$ , with colors ranging from the blue through the first detection of a very red LSB galaxies ( $B-V = -0.7$  to  $1.7$ ). The  $M_{HI}/L_B$  of these galaxies ranges from  $0.1 M_\odot / L_\odot - 50 M_\odot / L_\odot$ , showing this sample to range from very gas poor to possibly the most gas rich galaxies ever detected.

One of the more intriguing results of this survey is that the galaxies with the highest  $M_{HI}/L_B$  correspond to some of the reddest (optically) galaxies in the survey, raising the question of why star formation has not continued in these galaxies. Since the average H I column density in these systems is above the threshold for massive star formation, the lack of such may indicate that these galaxies form some kind of “optical core” which trace a much more extended distribution of neutral hydrogen. Alternatively, a model in which no stars more massive than two solar masses form in these systems can explain the presence of both blue and red gas rich LSB galaxies. Moreover, under this model the baryonic mass fraction ( $f_b$ ) of LSB galaxies is the same as for galaxies of higher surface brightness, thus perhaps escaping the dilemma proposed by McGaugh & de Blok (1997a, 1997b) with respect to LSB and high surface brightness galaxies defining the same Tully-Fisher relation.

A subset of the detected LSB galaxies have rotational velocities  $\geq 200 \text{ km s}^{-1}$  and yet are at least an order of magnitude below  $L_*$  in total luminosity. As such, they represent extreme departures from the standard Tully-Fisher relation. In fact, our sample does not appear to have any significant correlation between the velocity widths and absolute magnitudes, with only 40% of the

galaxies falling within the  $1\sigma$  low surface brightness galaxy Tully-Fisher relation. Overall, the discovery of very red, sub- $L_*$  but very gas rich LSB galaxies in the nearby Universe has increased, once again, the overall parameter space occupied by disk galaxies.

*Subject headings:* galaxies: formation – galaxies: evolution – galaxies: distances and redshifts – galaxies: color – galaxies: mass – galaxies: structure

## 1. Introduction

Our knowledge of the local galaxy population, and by inference the total galaxy population, has been biased towards the bright, high surface brightness (HSB) galaxies found in our current galaxy catalogs. Low surface brightness (LSB) galaxies, those systems with central surface brightness lower than the natural sky brightness cannot, however, be ignored, as they are both a significant contribution to the total mass found in galaxies and are critical to our understanding of the distribution of galaxy types. Without adequate representation of the LSB class of galaxies we can not fully uncover the range of evolutionary paths available for galaxies to follow. LSB galaxies are important in a number of other contexts as well:

- While the overall space density of LSB disks remains unknown, significant numbers of galaxies with  $\mu_B(0) \geq 24.0$  mag arcsec<sup>-2</sup> have been detected in CCD surveys, suggesting that the trend remains fairly constant (O’Neil *et.al.* 1997b) or even rises towards fainter  $\mu_0$  (Schwartzzenberg *et.al.* 1995, Dalcanton *et.al.* 1997). As a result, there is a strong possibility that LSB galaxies are the major baryonic repository in the Universe (i.e. Impey & Bothun 1997; O’Neil & Bothun 1999).
- Increasing the space density of galaxies at  $z = 0$ , in principle, poses a feasible solution to the dilemma of the apparent excess of faint blue galaxies at intermediate redshifts. While there is much to be worked out in the details of such a solution (see Ferguson & McGaugh 1995), the discovery of faint, red,  $z=0$  LSB spirals by O’Neil *et.al.* (1997b) is promising in this regard.
- Measurements of the LSB rotation curves by Pickering *et.al.* (1997) and McGaugh & de Blok (1997a) have yielded the result that the fundamental shape/mass density of the dark matter halo appears to be different in LSB galaxies compared to HSB

galaxies of the same circular velocity. Additionally, these rotation curves have shown that the baryonic mass fractions ( $f_b$ ) in LSB galaxies is, on average, a factor of 3 lower than HSB galaxies of the same circular velocity. These observations suggest that LSB and HSB disks are fundamentally distinct with the distinction being physically defined by differences in their respective halos.

Although a coherent picture of the underlying mechanism of LSB formation and evolution has not yet been found, previous studies have shown that most of the initial, and somewhat naive, concepts of LSB galaxies are at odds with the observations. For example, the idea that LSB galaxies are “faded” versions of HSB galaxies due to the dimming of an aging stellar population is shown by the optical colors, metallicity, and gas content of LSB galaxies to be completely wrong (Bell, *et.al.* 1998; McGaugh 1994; Schombert, *et.al.* 1990; van der Hulst, *et.al.* 1993). In addition, the measured low H I surface densities (van der Hulst *et.al.* 1993) in LSB galaxies raise the important question: Why are there any stars in these systems at all (i.e. O’Neil *et.al.* 1998; McGaugh & de Blok 1997b; O’Neil, Verheijen & McGaugh 1999)?

A recent survey by O’Neil, *et.al.* (1997a,b) has extended the known range of properties of LSB galaxies, including the discovery of an intriguing new class of fairly red LSB disks whose overall color is, in fact, quite consistent with a conventional fading scenario. As this survey contains LSB galaxies with a wide range of properties, i.e. colors from the very blue through the very red, scales lengths ranging from 1-4 kpc, central surface brightnesses from near the Freeman value ( $\mu_B(0) = 22.0 \text{ mag arcsec}^{-2}$ ) through  $\mu_B(0) = 25.0 \text{ mag arcsec}^{-2}$ , further study of this catalog presents an excellent opportunity for understanding the global properties of LSB systems. In particular, the complete properties of the LSB galaxies discovered by O’Neil *et.al.* (1997a,b) could not be ascertained as no redshift measurements existed. To further elucidate the nature of this new LSB sample, we undertook to detect

the entire catalog of O’Neil, *et.al.* (1997a,b) with the refurbished Arecibo Gregorian telescope.

The layout of this paper is as follows: In section 2 the observations, data reduction, and analysis is discussed. Section 3 describes the data analysis and presents the basic observational parameters which can be derived from the radio and optical observations. Section 4 briefly describes some new inferences on the star formation history of LSB spirals that can now be made with the discovery of red, but very gas rich, LSB galaxies. Finally, section 5 discusses how the types of LSB galaxies discussed here do not readily conform to the standard Tully-Fisher relation as defined by samples of cluster spirals. Concluding remarks are contained in section 6.

## **2. Observations and Data Reduction**

### **2.1. Observations**

Using the refurbished Arecibo Gregorian telescope we attempted detection of the complete list of LSB galaxies in the catalog of O’Neil, Bothun, & Cornell (1997a) (OBC from now on) available to the Arecibo sky. Data was taken using the L-wide and L-narrow receivers, both with 2 polarizations, 1024 channel sub-correlators, and 9 channel sampling. Each of the four sub-correlators has a 25 MHz bandpass, resulting in 5.2 km/s resolution (at 1420 MHz). The L-narrow receiver ranged from 1370 MHz – 1432.5 MHz and was centered at 1401.25 MHz, providing an overlap of two correlators across most of the spectrum and thereby effectively doubling the integration time. The L-wide receiver was centered at 1392.5 MHz with a range from 1350 MHz – 1435 MHz, resulting in only a 5 MHz overlap on each side. In both cases the overlap more than eliminated any problems which otherwise

may have arisen due to poor performance in the outer 50 channels of each correlator. During the observations the L-narrow receiver was set to linear polarizations (A or B) while the L-wide was set to circular polarization ( $A \pm iB$ ).

The data were taken between 24 June 1998 and 27 April 1999. A minimum of one 5 minute ON/OFF pair was taken of each galaxy, followed by a 10 second ON/OFF calibration pair. When possible, if a galaxy remained undetected after the first 5 minute pair and that galaxy was either particularly interesting (very low  $\mu_B(0)$  or high B–V), and/or looked like a potential detection, at least one (and on occasion many) more 5 minute ON/OFF pair was taken of it. Table 1 lists the total number of observations done on each galaxy, as follows: Column 1 lists the galaxy name; Columns 2 and 3 give the right ascension and declination (in B1950 coordinates) of the galaxies as determined from the digital sky survey (DSS); Columns 4 and 5 list the number of 5 minute pair taken with each receiver. If the pairs were of a different length of time (i.e. 2 minutes), that time is given in parenthesis; Column 6 lists whether or not a galaxy was detected.

## 2.2. Galaxy Identification

All data was analyzed using the ANALYZ software package (Deich 1990). The two polarizations, as well as any overlapping channels were initially combined to determine whether or not a detection had occurred. Once an initial detection was made, each polarization and (when the detection lay within more than one sub-correlator) each sub-correlator was analyzed to insure the galaxy could be retroactively detected within each system, providing a minimum of 2 – 4 semi-independent detections and minimizing the chance of false positives (i.e. RFI noise).

After a detection was confirmed, the two polarizations (3-channel boxcar and hanning

smoothed) of each observation of that galaxy were combined, and the resultant data displayed against correlator channel. To avoid possible problems resulting from a gain loss in the outer 50 channels of each sub-correlator, any detection which lay within 100 channels of a sub-correlator edge was not used, as there was always enough overlap in the sub-correlators for at least one ‘clean’ galaxy image. Otherwise each sub-correlator detection was analyzed individually and the results were averaged. In the cases that more than one observation of a galaxy existed, and the detection in question had a low S/N, the multiple observations were averaged before the above process was applied. If more than one observation of the galaxy under study was available yet the S/N was high enough within only one ON/OFF pair for reliable analysis, each observation was analyzed separately with the averaged results being recorded in Table 2.

### 2.3. Gain/Zenith Angle Correction

Corrections had to be applied to the data to accommodate variations in the gain and system temperature of the telescope with zenith angle. The correction was determined through tracking a number of previously studied continuum sources the entire time they were visible to the Arecibo sky ( $z_a < 19.6^\circ$ ). The obtained fractional temperatures ( $\frac{ON}{OFF} - 1$ ) were fit against the known values, as published in the NRAO VLA Sky Survey (Condon, *et.al.* 1998). Eight sources were observed with the L-narrow receiver and seven with the L-wide receiver between 01 June through 14 June, 1998. Fourth-order best fit curves were found for this data and the gain and temperature variance, with zenith angle, was obtained for each receiver.

To insure any observed difference in G/T between the L-wide and L-narrow receivers was systematic, five of the continuum sources observed with the L-wide receiver were

subsequently observed with the L-narrow, and the ratio of fractional temperatures versus zenith angle were determined. The result is a linear plot which shows slight systematic variation with zenith angle, L-wide having the lowest sensitivity at low zenith angles. The average of the plot for all five continuum sources is  $\frac{L-wide}{L-narrow} = 0.840 \pm 0.002$  ( $3.0^\circ < za < 18^\circ$ ).

As a final check, we interspersed observations of a subset of galaxies from the catalog of Lewis, Helou, & Salpeter (1985) with the LSB galaxy survey described in this paper. On average our L-narrow results differed from those of Lewis, Helou, & Salpeter by  $2.9 \pm 0.7\%$ , Those with the range in differences being  $-2\%$  to  $10\%$  of their value. The L-wide was comparable, with an average offset of  $7.1 \pm 1.5\%$  and a range of  $-12\% - 18\%$ . See Lewis, *et.al.* (1999) for further details.

## 2.4. Data Reduction

Baselines were fit to the data using a modified version of the GALPAK BASE module, which fits a polynomial to all the data within a specified region. For this data we let the polynomial vary in order from 1–5 for the region lying within 100–150 channels on either side of the galaxy edges. The most sensible best fit line (typically of order 1) was then used as the baseline subtraction. Again, that region within 100 channels of a sub-correlator edge was avoided for this analysis.

Once the baselines were subtracted, the velocities were corrected to the heliocentric coordinate system and the velocity, velocity widths, and the flux of the H I profiles were determined. In each case, the values were found four ways – at 20% of the mean profile flux, at 50% of the mean profile flux, at 20% of the peak flux, and at 50% of the peak flux. (As a fraction of the detected galaxies do not show a two-horned profile, no attempt was

made to incorporate horns into the data analysis.) During the flux analysis, galaxy edges were estimated by eye. Although this introduces some measurement error, the error lies well below the 5 – 10 km/s width error which exists due to the somewhat low S/N in the 21-cm data.

## 2.5. Error Analysis

Error analysis was done as follows – as no difference existed between the fluxes determined using the four methods listed above, the determined flux errors are completely derived from the analysis of HSB galaxies in the catalog of Lewis, Helou, & Salpeter (1985). Thus the L-narrow fluxes are given errors of  $\pm 5\%$  while the fluxes determined from L-wide data have 10% errors. It is important to note that, as determined from the Lewis, Helou, & Salpeter (1985) galaxies, it is possible that the flux errors are systematic, and result in our presenting too low a value for  $M_{HI}$ .

Comparing our central velocity values with those of Lewis, Helou, & Salpeter (1985) shows virtually no error (the highest error being 1%), showing there is no significant contribution from systematic errors. The low S/N and lack of symmetry for the galaxies in this survey, though, did result in a typical scatter between the four different velocity measurements of  $\pm 2 \text{ km s}^{-2}$ , on average. If the error was larger, it is noted in Table 2.

The low S/N and asymmetric profiles of the LSB galaxies in this survey also resulted in considerable scatter in the velocity width measurements. Comparing our results with Lewis, Helou, & Salpeter (1985) suggests our data may have systematically wider profiles by 1 – 2 %. Additionally, there was a typical scatter between the two width determinations (peak and mean) for each fraction (20% and 50%) of 3%, resulting in a total 5% error for the widths (again unless otherwise noted in Table 2). As discussed in Bothun & Mould

(1987), errors in 21-cm line width measurements are likely the dominant source of observational scatter in the Tully-Fisher relation. This problem is made worse if most of the H I profiles do not have very steep sides. A quick perusal of Figure 1 immediately suggests that line width errors are larger than “normal” for this sample.

### 3. The Detected Galaxies

#### 3.1. The Data

The information obtained from the observations described herein are listed in Table 2 and are arranged as follows. All 21-cm profiles are shown in Figure 1.

**Column 1:** The galaxy name as it appears in OBC.

**Column 2:** The morphological type of the galaxy, as determined from the optical images of OBC.

**Column 3:** The heliocentric velocity of the galaxy in  $\text{km s}^{-1}$ , determined as described above. The listed velocities have errors of  $\pm 5 \text{ km s}^{-1}$ , unless otherwise noted.

**Column 4:** The apparent (Johnson) B magnitude for the galaxies, as given in OBC. The error, also as given in OBC, is  $\pm 0.1$ .

**Column 5:** Absolute B magnitude, determined using

$$M - m = -25 + 5\log(H_0) - 5\log(cz) - 1.086(1 - q_0)z \quad (1)$$

(Weinberg 1972). For this, and all other derivations in this paper,  $H_0=75 \text{ km s}^{-1} \text{ Mpc}^{-1}$ ,  $c=2.99793 \times 10^5 \text{ km s}^{-1}$ , and  $q_0=0.1$ . No k-correction was applied as it would be less than

0.1 mag.

**Columns 6 & 7:** The average uncorrected velocity widths at 20% and 50% of the peak and mean flux. Errors are  $\pm 10 \text{ km s}^{-1}$ , unless otherwise noted.

**Column 8:** The total flux, after correction for gain and temperature variances with zenith angle. No correction for partial resolution was made although from the asymmetric appearance of some of the profiles (e.g. P3-3, P5-4) it is possible there was some degree of poor pointing.

**Column 9:** The total H I mass, in  $10^8 M_\odot$ , as found from

$$M_{HI} = 2.356 \times 10^5 D^2 \int S_\nu d\nu M_\odot \quad (2)$$

where the distance is in Mpc and the flux ( $S_\nu$ ) is in  $\text{Jy km s}^{-1}$ .

**Column 10:** The H I mass to luminosity ratio in units of  $M_\odot / L_\odot$ , where the luminosity was determined from the magnitude listed in column 4.

**Column 11:** The H I mass to luminosity ratio in units of  $M_\odot / L_\odot$ . In this case the luminosity was determined through the total integrated blue magnitude ( $m(\alpha)$ ) given in OBC and converted to absolute magnitude using Equation 1.

**Column 12:** The B–V color as given in OBC.

**Column 13;** The galaxy’s optical inclination, determined from the OBC data using the IRAF ELLIPSE parameter. The inclination listed is simply  $i = \sin^{-1}(r_{minor}/r_{major})$  The inclination error is  $\pm 5^\circ$  unless otherwise noted.

### 3.2. The Non-Detected Galaxies

Table 3 lists all of the galaxies for which the attempts at detection failed during this survey. Column 1 of the table gives the galaxy name, while Columns 2 and 3 provide the  $1\sigma$  detection limits for both the L-narrow and the L-wide set-ups, found from the r.m.s. error in the baselines. It is likely that were a galaxy to lie at least  $1.5\sigma$  above the baseline it would have been detected. It is important to note, however, that this simply limits the maximum H I density of the undetected galaxies *if they lay within the 0 – 11,500 km s<sup>-1</sup> survey boundary*. As many galaxies were found near the 11,500 km s<sup>-1</sup> survey boundary, it is quite possible that a planned search at higher redshift will readily detect many of the ‘missing’ galaxies.

### 3.3. Galaxy Distribution

The distribution of the galaxies in the survey follows the large-scale HSB galaxy distribution. Figure 2 shows a cone diagram for all the galaxies in Pegasus and Cancer fields of OBC with known velocities (obtained either through this survey or through NED, the NASA Extragalactic Database). As can be readily seen, all the galaxies lie within the HSB defined galaxy clusters, and none of the detected galaxies fill in the cluster voids. The one exception is U1-4 (not shown) which appears to be a genuine isolated system. That none of the detected galaxies fill in the cluster voids is in agreement with both the result of Schombert *et.al.* (1995) for LSB galaxies off the Second Palomar Sky Survey and the Uppsala General Catalog search by Bothun, *et.al.* (1986). The reader should also note that these galaxy clusters do not match the extreme regions of galaxy density, such as the Coma or Virgo clusters. We make no statement on existence of LSB galaxies in cluster cores, already shown to be rare by Bothun *et.al.* (1993).

A follow-up study into the clustering statistics of all these galaxies (O’Neil & Brandenburg 1999) should clarify this issue. For now it suffices to note that no trend was found between a galaxy’s velocity or cluster identity and its color, surface brightness, rotational velocity, inclination, and absolute magnitude. It is interesting to note that with the inclusion of our LSB galaxies, galaxy groups now found to contain the full range of galaxy types, from dwarfs to intrinsically luminous LSB galaxies, and from the very blue, star-forming galaxies to those galaxies with apparently old stellar populations.

### 3.4. Galaxy Photometry, Morphology and Structure

The galaxies for the sample span a range of morphological types from late-type spiral to dwarf irregulars. The Hubble types are given in Table 2, following the prescription of Schombert, Pildis, & Eder (1997) and Sandage & Binggeli (1984). This system is based mostly on the presence, and size of a bulge component. Objects with a distinct bulge are classed Sb to Sc depending on bulge dominance. Objects with a disk-like shape and some central concentration are classed as Sm. Objects with no shape or concentration are classed as Im. Most of the objects with double-horned H I profiles, indicative of rotation, displayed disk-like morphological appearance. Eight of the 43 objects (19%) are classed as Im or dwarf-like. All of these dwarf galaxies have luminosities and sizes on the low end of the sample scale, justifying their classification as dwarf in terms of size and magnitude. Several of the disk galaxies in the sample have magnitudes and scale lengths comparable to the class of dwarf spirals (Schombert *et.al.* 1995), but many also have rotational masses similar to the most massive disk galaxies known (see Section 5). This immediately suggests detection of objects that strongly violate the Tully-Fisher relation.

Figures 3 and 4 compare  $M_B$  with the total neutral hydrogen mass, color, central surface

brightness, and scale length for all the galaxies detected with our survey. In Figure 3 these results are compared with other samples (de Blok, van der Hulst, & Bothun 1995; de Blok, van der Hulst, & McGaugh 1996; Schombert, *et.al.* 1995; Matthews, & Gallagher 1997; Bothun, Sullivan, & Schommer 1982; Becker, *et.al.* 1988). The most relevant comparison might be with Bothun (1982) who reported the results for normal spirals in the Pegasus and Cancer regions. With respect to Figure 3a, our sample clearly defines the same locus of points with the obvious exception of 3 outliers – C1-2, C5-5, and N9-2 (having extremely high  $M_{HI}/L_B$  ratios). However, most of the points sit above the ridge line fit to these samples, indicating that, on average, our sample galaxies have higher gas to star ratios. The situation summarized in Figure 3b however is quite different. Here we can see that our sample has clearly extended the color-magnitude relation for spiral galaxies with gas in that we have detected a number of red galaxies with luminosities below that of  $L_*$ . Previous reports of very red gas-rich disk galaxies (e.g. Schommer & Bothun 1983, van der Hulst *et.al.* 1987) have all been relatively luminous spirals. To our knowledge, this survey is the first to have discovered red, gas-rich objects of relatively low intrinsic luminosity. Overall, however, there clearly is no color-magnitude relation defined for the late type samples shown here. These objects clearly define a very diverse galaxy population.

In Figure 4a we plot the absolute B magnitude versus  $\mu_B(0)$  for the galaxies in this survey. By selection, there are no galaxies with  $\mu_B(0)$  brighter than 22.0 mag arcsec<sup>-2</sup>. The void in the top right corner is most likely artificial, created by the inability of OBC to identify small, compact galaxies (the ‘star-like galaxies’ of Arp 1965). Had high enough resolution images been taken by OBC, that corner might disappear. Indeed, that corner is often inhabited by blue compact dwarfs which have become the source of intense recent study (e.g. Marlowe *et.al.* 1999). The more interesting void in Figure 4a is at the lower left corner. This is the region where very LSB yet intrinsically very luminous, and physically quite large, galaxies would lie (the Malin I galaxies). This lack of intrinsically luminous,

very LSB galaxies can also be seen in Figure 4b, which shows a void in the very LSB, large scale length regime. This result either shows that the intrinsic space density of these physically large LSB disks is low (but see Sprayberry *et.al.* 1995a) or that we have not sampled the correct regions to find them; that is, they tend to avoid the extended cluster environment (see Hoffman, Silk, & Wyse 1992) are only found in isolated, very low density environments.

#### 4. Red Gas Rich LSB Galaxies

The use of the color-gas content plane as a diagnostic for studying the evolution/star formation history of galaxies was pioneered by Tinsley (e.g. Tinsley 1972). Bothun (1982) present a codified version of this as it applies to cluster spirals. One of the main results of that analysis was that, for a sufficiently large sample of spirals, there really was no correlation between disk color and the gas-to-star ratio. Figures 5 a and b show the H I mass and  $M_{HI}/L_B$  versus  $B - V$  color for the galaxies in our survey where we confirm the absence of any correlation. Note the presence of some galaxies in our sample which have extreme values of  $M_{HI}/L_B$ . More to the point, our samples clearly shows that there is no definitive trend toward lower  $M_{HI}/L_B$  or  $M_{HI}$  with redder colors. In fact, if a trend does exist, it is toward *higher* H I mass and  $M_{HI}/L$  with increasing  $B-V$ , raising an interesting question – if a galaxy has been capable of forming and evolving at least one generation of stars to reach  $B-V \geq 1.0$ , and the galaxy still contains a significant fraction of neutral hydrogen, why has it been unable to continue this process? That is, why hasn't such a disk exhausted its gas and assumed its endpoint evolution in this diagram at the lower right where the bulk of S0 galaxies reside? Clearly, we have detected what could best be described as a “dormant” population of disk galaxies.

One solution to the above questions may be found by appealing to Kennicutt’s (1989) argument that a critical density of gas must be present for star formation to occur. Thus it could be argued that star formation in these red, high  $M_{HI}/L_B$  galaxies occurred only in those regions dense enough to support it, and that the bulk of the gas is located in the less dense regions which have been unable to commence self-gravitation. In this case, these galaxies would represent “optical” cores inside a much more extended gas distribution. Certainly individual examples of this have been found (e.g. NGC 2915 – Meurer *et.al.* 1996), but these seem to be quite rare. Indeed, a systematic search for such kinds of objects from a seed sample of blue compact dwarfs failed to detect any examples of large H I mass objects with small optical sizes (i.e. Salzer, *et.al.* 1993).

Previous studies of red, H I rich disk galaxies (e.g. van der Hulst *et.al.* 1987) have shown them to be large scale length objects with generally strong color gradients. Their overall properties imply that the bulk of the star formation has occurred within the inner two scale lengths and the gas at larger radii is mostly unprocessed. The red H I rich galaxies in this survey, however, are not of large scale length as shown in Figure 6. In fact, for the extreme cases, it can be seen that the galaxies with  $M_{HI}/L_B \geq 9 M_\odot / L_\odot$  are confined to the  $\alpha < 2$  kpc range. Possibly this is an indication that these galaxies are indeed “optical” cores of a much larger H I extent. However, if their H I size is similar to their optical size then we have discovered a class of relatively compact galaxies which have an average column density of approximately  $10^9 M_\odot / 100 \text{ kpc}^2 = 10^{21}$  atoms per  $\text{cm}^{-2}$  (e.g. above the threshold), but which are not forming stars, or at least are not forming massive stars. It is this latter possibility that makes the discovery of these objects relevant to the apparent contradiction discussed by McGaugh & de Blok (1997a) regarding the low  $f_b$  value that results for LSB galaxies if they are fit with a standard dark matter halo.

This low  $f_b$  value follows directly from assuming a low M/L for the stellar population.

Typically a value of  $(M/L)_B$  of 1–2 is assumed as this is consistent with the relatively blue colors of the McGaugh & de Blok disks. But what if this is wrong? What if we are dealing with an anomalous stellar population because of an anomalous IMF? Suppose, for the sake of argument, that we force the  $f_b$  to be the same for both LSB and HSB galaxies. One motivation for doing this is to better understand why it is that LSB disk galaxies apparently define the same Tully-Fisher (TF) relation as HSB disk galaxies (e.g. Sprayberry *et.al.* 1995b; Zwaan *et.al.* 1997). This issue has been addressed by Dalcanton *et.al.* (1997), Mo, Mao, & White (1998) and Steinmetz & Navarro *et.al.* (1999) who can recover this “universal” TF relation by assuming that galactic disks are sub-maximal and it is the halo properties that therefore dominate the mass profile. Support for this general picture comes from a recent study by Courteau & Rix (1999) who show that the TF relation and its scatter are best understood if the disks of HSB spirals are indeed sub-maximal. On the other hand, Beauvais & Bothun (2000) present fairly compelling evidence that disks are likely maximal (see also Sackett 1997; Giraud 1998).

Mo, Mao, & White (1998) explore the efficiency of the conversion of baryonic mass into stars. Variations in this efficiency can obviously lead to different loci of points in the TF relation. In the extreme case of no conversion into stars, obviously a galaxy has no luminosity to even place it on the TF relation! Mo, Mao, & White (1998) find that surface mass density is a key parameter in determining this efficiency (see also Bothun 1990) and predict that low surface mass density systems have low efficiencies leading to the existence of relatively gas-rich but dim galaxies. Such galaxies, are in fact, the kind that we have discovered here.

However, the luminosity evolution of galaxies depends on factors other than the efficiency of gas to star conversion. There is the critical issue of the mass function of stars that are formed during the conversion process. While discussing whether or not there is a universal

IMF is well beyond the scope of this paper, we amplify the issue that was initially raised in McGaugh and de Blok (1998) – at face value, the data seem to argue that two potentials of much different baryonic mass fraction, but similar circular velocity, produce the same amount of light (hence making a universal TF relation). While this issue can be resolved using Modified Newtonian Dynamics (MOND e.g. Milgrom 1983), that solution seems no more extreme than a solution which seeks to change the stellar population so that the baryonic mass fractions in LSB galaxies in fact, is the same as in HSB galaxies.

For  $f_b$  to be the same, the assumed  $(M/L)_B$  for blue, LSB disks would have to be 10, instead of 1–2. While there may be some dynamical constraints of having  $(M/L)_B$  this high (Quillen & Pickering 1997), values this large cannot be explicitly ruled out for the objects in the de Blok and McGaugh (1998) sample. They are only indirectly ruled out by the standard  $(M/L_B)/B - V$  arguments which flow from an assumed IMF. Therefore, one is obligated to produce a stellar population which basically has  $(M/L)_B \sim 10$  (the value for a typical elliptical galaxy) and  $B - V \sim 0.3$ . This is a tough problem and its solution requires an extreme stellar population, one that is presently deficient in stars on the giant branch, so that the high  $(M/L)_B$  is provided by main sequence stars of mass less than  $0.3 M_\odot$  and the blue colors are supplied by a small amount of A and F stars. This population of A and F stars must remain sufficiently small so that their subsequent giant branch evolution does not significantly alter  $(M/L)_B$ . Note that a galaxy with such a stellar population will not remain dim forever, only for the first few billion years of its life. After 10 Gyr, the heavily populated lower main sequence will begin to evolve onto the giant branch and the luminosity will increase.

This extreme model, in fact, is observationally testable if near IR colors could be obtained. Dwarf dominated integrated light will be significantly bluer than giant dominated integrated light in  $V - K$ . We also note that it is very difficult to produce any stellar

population with giant branch dominated light that has  $B - V \geq 1.0$  (see Tinsley 1978; Bothun 1982) and ages that don't exceed 12 Gyrs. The reddest objects in our sample approach  $B - V = 1.2$ . Since there is unlikely to be significant internal extinction in these systems (see below), these very red colors imply either 1) a rather old galaxy (unlikely) or 2) the presence of very cool giants usually only seen in metal-rich populations (again unlikely), or 3) a large contribution to the light from main sequence stars of spectral type K5 – M0.

In the galaxies' star forming (ON) state it is blue. In the galaxies non-starforming (OFF) state it fades and reddens. In Table 4, we present three models (discussed in detail below) which show the ON and OFF states that can be achieved under our dwarf dominated integrated light scenario. While this scenario is clearly non-standard it does produce both red and blue gas-rich LSB galaxies with high values of  $M/L$  in both cases. As such, this scenario provides an alternative to apparent significant discrepancy between the different  $f_b$  values inferred for LSB and HSB disks. However, to be fair, in reaching this conclusion, McGaugh & de Blok (1997a,b) actually compare the  $f_b$  of LSB disks with clusters of galaxies, which typically have  $f_b$  in the range 0.1-0.3 (e.g. the baryon catastrophe – see White *et.al.* 1993). By contrast, LSB disks are factor of 3-5 lower. Direct comparison to HSB disks, however, is more problematical as most rotation curves don't go out far enough to accurately sample the halo. Thus,  $f_b$  depends upon the scale of measurement in the HSB sample. Adding to the confusion are the results of Zaritsky *et.al.* (1997) whose work on satellite galaxies and the total extent of the halos around HSB galaxies leads to  $f_b \approx 0.05$ , similar to those of LSB disks but significantly less than what is seen in clusters. So while its clear that  $f_b$  for LSB disks is significantly lower than that measured for clusters of galaxies, it remains ambiguous whether or not  $f_b$  is also significantly lower compared to individual HSB disks.

This lack of clarity on the  $f_b$  issue, however, does not deter us from pursuing our alternative stellar population model. Indeed, in a rigorous but now largely forgotten paper, Larson (1986) makes a set of compelling arguments about the need for a bi-modal IMF to fully reconcile the chemical evolution of galaxies with their observed colors and mass-to-light ratios. One of those modes involves a peak at  $M \sim 0.25 M_\odot$  and that is the mode we have adopted as the dominant mode of star formation in our models. To account for the presence of very blue LSB galaxies and the observation (e.g. McGaugh 1994) that some LSB galaxies have a small number (e.g. 1–6) of H II regions we have added a few O,A and F stars to this mode. However, as pointed out in de Blok (1997) as well as O’Neil *et.al.* (1998), there is ample evidence that LSB disks are generally deficient in the formation of massive stars. The models of O’Neil *et.al.* (1998) assert that this deficiency is a statistical result of a low surface density of gas and the difficulty of gathering sufficient gas mass over a relatively small spatial scale to produce the kind of massive star formation that is observed in HSB disks.

Under this set of assumptions we ran a large series of models and show the results for 3 specific cases in Table 4. In each case, the ON state is achieved by allowing  $\sim 2\%$  of the available gas mass to participate in star formation. Values for  $B - V$  and  $M/L$  for the stellar population are listed for the ON and OFF states. The extreme nature of these models is readily apparent as the giant branch contribution to the integrated light at B is never larger than 10%. In models 1 and 2 we truncate star formation at  $2 M_\odot$  so that only A and F stars are produced. The main difference between the two models is that model 2 peaks at a lower main sequence mass to drive the colors as red as possible. Still, none of our models can reach the more extreme  $B - V$  values in this sample (e.g.  $B - V \geq 1.2$ ). In model 3, we add O-stars to model 2 in order to accommodate the existence of the observed H II regions. This addition does not appreciably lower the  $M/L$  for the stellar population but does push the  $B - V$  color blueward by  $\sim 0.1$  magnitude. Since only a relatively small

amount of gas is involved in the OFF to ON transition, then our models suggest that both blue and red H I rich LSB galaxies can co-exist for billions of years, given their amounts of available H I. Note as well that in all three cases, the integrated light in the ON state is dominated by the small number of O,F and A stars. As the light from these stars fades, the luminosity of the galaxy will decrease by a factor of 3-4 and the galaxy will return to its red OFF state. In fact, if in its ON state the galaxy falls on the standard TF relation, it will surely be well below this position as it transitions to the OFF state. In the next section, we will show that these red H I rich LSBs are significantly under-luminous with respect to their circular velocity.

We have pursued this alternative stellar population model strictly as means of determining the plausibility of producing a stellar population which can be blue ( $B - V \sim 0.4$ ) but which can have a significantly higher  $M/L$  ratio so as to raise the value of  $f_b$  for LSB disks to the level observed for clusters of galaxies. The models presented in Table 4 achieve this and we leave it up to the reader to assess their plausibility in comparison to other alternatives (e.g. a non-universal value for  $f_b$ , MOND, etc).

Clearly, further resolution of this intriguing matter requires actual measurements of the H I distributions in these red H I rich objects. Either the gas is well below the critical density thus effectively shutting off star formation, or star formation is proceeding without the accompanying massive star formation. While that would be very strange, we argue that the position of these galaxies in the color-gas content plane is already very strange so something quite different is likely going on. The fact that we can produce blue LSB galaxies in a model in which only 2% of the gas supply needs to participate in a star formation event is consistent with what appears to be occurring in UGC 12695, perhaps the bluest LSB detected to date. UGC 12695, in fact, has a total H I mass remarkably near its total dynamical mass ( $M_{HI} = 4.2 \times 10^9 M_\odot$ ,  $M_{dyn} = 9.6 \times 10^9 M_\odot$ ), yet recent HST

Wide Field Planetary Camera-2 and VLA observations show that the majority of star formation in UGC 12695 is occurring in isolated regions. Thus, although UGC 12695 has a high total H I mass, the surface density of the gas is often below the Kennicutt star formation threshold (O’Neil, Verheijen, & McGaugh 1999; O’Neil, *et.al.* 1998). If the light from this small amount of star formation fades, its quite likely that UGC 12695 would be a red, LSB, H I rich object.

## 5. Deviations from the Tully-Fisher Relation

In 1977 Tully & Fisher published an empirical correlation between galaxies’ H I velocity width and their absolute magnitude (or diameter). Since that time the Tully-Fisher (TF) relation has been used in over 100 different investigations that attempt to determine the relative distances between disk galaxies and/or clusters of galaxies. This multitude of different investigations clearly establishes that the TF relation exists in a variety of different samples. The recognition that the potentials of disk galaxies are dark matter dominated makes the existence of the TF relation very difficult to understand from first principles because, apparently, it requires that the amount of luminosity trace the dark matter in a way that scales exactly with  $V_c$ . This fine tuning, in essence, requires that the value of  $f_b$  in disk galaxy potentials be nearly constant. The required constancy of  $f_b$  should be a troubling point. The existence of the TF relation implies that just enough baryonic gas creeps into these dark potentials and then has the correct star formation history to produce the right amount of light for a given circular velocity. Worse still is the apparent physical dilemma or paradox that results from the apparent ability for samples of LSB and HSB spirals to define the same TF relation. Simple virial arguments coupled with the constancy of  $M/L$  fail to reproduce this observation if LSB and HSB disk galaxies are dominated by dark matter halos of the same form (see Bothun & McGaugh 1999). The

only way out of this dilemma is to postulate that fine tuning exists between central surface brightness and  $M/L$  in such a way so as to preserve a universal TF relation.

In this section, however, we will document how our, relatively extreme sample of LSB galaxies, in fact does not conform well to the standard TF relation. While hints of this have been seen in other samples (e.g. Matthews, van Driel, & Gallagher 1998) those hints are mostly based on behavior at the low line width end. Our sample contains galaxies with substantial circular velocity that nevertheless strongly deviate from the TF relation.

### 5.1. Inclination, Extinction, and Random Motion Corrections

To compare our results with those of previous galaxy surveys, we modeled our magnitude and line width corrections after those of Tully & Fouque (1985) and Zwaan, *et.al.* (1995). Thus we corrected the magnitudes for Galactic and internal extinction to face-on orientation, using

$$B^i = B + 2.5 \log \left( f \left( 1 + e^{-\tau/\cos(i)} \right) + (1 - 2f) \left( \frac{(1 + e^{-\tau/\cos(i)})}{\tau/\cos(i)} \right) \right) \quad (3)$$

with  $\tau=0.55$  and  $f=0.25$ . The line widths were corrected for random motion effects and inclination, using

$$W_{50c}^i = \sqrt{\left( W_{50}^i{}^2 + W_t^2 - 2W_{50}^i W_t \left( 1 - e^{-(W_{50}^i/W_t)^2} \right) - 2W_t^2 \left( e^{-(W_{50}^i/W_t)^2} \right) \right)} \quad (4)$$

with  $W_{50}^i = W_{50} (\cos(i))^{0.22}$  and  $W_t$ , the turbulent motion parameter, being set to 14 km s<sup>-1</sup>.

Figure 7(a) shows  $W_{50c}^i$  versus  $B^i$  with the  $1\sigma$  and  $2\sigma$  ranges of Zwaan, *et.al.* overlaid on the plot. The Zwaan, *et.al.* data, based off Broeils (1992) findings, is

$$M_{B_{corr}} = -6.59 \log(W_{50_{corr}}) - 3.73 \pm 0.77 \quad (5)$$

Only 77% of the data falls within the  $2\sigma$  lines of Zwaan, *et.al.* , and a mere 40% fall within the  $1\sigma$  lines. Clearly this sample does not produce a well-defined TF relation for LSB galaxies in the way that the sample of Zwaan *et.al.* does.

## 5.2. Potential Errors

Before delving into the significance of Figure 7(a), a further look into potential errors is required. The first question which needs to be addressed is that of potential biases introduced by above corrections, as all were done as if this sample was comprised of HSB galaxies.

The application of these “corrections” however, to LSB galaxies may be somewhat dubious. To begin with, there is a fair bit of evidence that suggests LSB galaxies have very low amounts of internal extinction and may, in fact, be extinction free. For instance, Sprayberry *et.al.* (1995b) did not apply any extinction corrections to the magnitude and formed a TF sample with a slope very near the virial slope of  $-10$ . The extinction correction assumes the galaxies are at least moderately optically thick. In Figure 8 we plot the  $B-V$  vs  $B-I$  colors of the galaxies in OBC. A nice locus of points is found whose position matches simple expectations of stellar population models. Where the red galaxies driven so by excessive amounts of dust we would observe significant shifts away from this relation. The tightness of the two color diagram thus provides another indication that LSB galaxies are relatively dust-free (Figure 8). Additionally, it should be noted that the six most deviant points in Figure 7(a) (P1-3, P9-4, C4-1, C5-5, C6-1, C8-3) range in color from  $B-V = 0.5 - 1.0$  and in inclination from  $45^\circ$  through  $73^\circ$  . It is therefore likely that, if anything, the extinction corrections applied to the data are larger than necessary, and the true B magnitudes are fainter than shown in Figure 7(a). This, then, would shift the data

points downward, and farther from the Tully-Fisher relation.

Perhaps a better gauge of the departure of our LSB sample from the standard TF relation is provided in Figure 9 which shows the I-band Tully-Fisher relation for the data in this paper, with the data and  $1\sigma$  lines from Pierce & Tully (1988) overdrawn. From this it can be seen that the scatter is as deviant in the I band as in the B for our data. It should be noted that the two data points (U1-4, and I1-1) which lie above Pierce & Tully's TF relation in Figure 9 all belong to galaxies which are not a part of any known cluster and hence we can not assign some mean "cluster" distance to these galaxies as we can for the bulk of the objects in our sample (see Figure 2).

The next correction was done to compensate for the inclination of the galaxies when trying to determine their rotational motion. This correction is fairly straightforward provided the true inclination of a galaxy is known. The inclination of the galaxies in this survey were determined by OBC assuming their true (face-on) shape is a perfect circle. LSB galaxies tend to be more amorphous in appearance than their HSB counterparts, however, making optical determinations of their true inclination difficult. By their very nature, LSB galaxies are difficult to fit isophotes to and there is a fair amount of variation in position angle and ellipticity between adjacent isophotes. While some of this noise averages out, there is likely an increase scatter in the TF relation for this sample just as a result of "inclination" noise. It is unclear, however, if there is any systematic effect present in applying the inclination correction to the measured line width. It should be noted that the  $\pm 5\%$  error in inclination is accounted for in the error bars of Figure 7.

The final correction undertaken was to compensate for the random motion of the gas contained within each galaxy. This is the most uncertain of all the corrections, as the parameter which describes the importance of turbulent motion,  $W_t$ , is unknown for LSB galaxies. For HSB galaxies,  $W_t$  appears to be of order 10-15 km/s, averaged over the entire

disk (see data in Beauvais & Bothun 1999). For LSB galaxies one might expect  $W_t$  to be larger due to the lower restoring force perpendicular to the disk (due to low surface mass density). On the other hand,  $W_t$  also is a measure of the kinematic feedback of star formation to the gas and LSB galaxies have quite low current star formation rates. Thus it is possible that  $W_t$  is either significantly greater than (or smaller than) that used in the above equations, which would shift the points in Figure 7 to the left (or right).

Since the application of our corrections to LSB galaxies may have limited validity, it seems worth just plotting the data without the corrections. This is done in Figure 7(b) which shows the same galaxies without the corrections for inclination, internal extinction, and random motions (only the Galactic extinction correction remains). The situation with respect to the uncorrected data, in comparison with the lines of Zwaan, *et.al.* (1995), is very similar to that in the corrected data, strongly indicating that the observed (large) deviations from the TF relation are real, and not the result of large systematic errors associated with applying the corrections.

### 5.3. Why no Tully-Fisher Relation?

The most obvious question to raise in regards to our results is why our survey did, and previous surveys did not, find galaxies deviating so widely from the Tully-Fisher relation. One possibility is simply the sensitivity of our survey and the size of this LSB sample. The combination of the large number of data points and the increased sensitivity of the Arecibo Gregorian system make for the ready detection of low S/N galaxies (i.e. P6-1 and P1-3). The second part of the answer to the above question is that the discovery of a group of galaxies which do not follow the Tully-Fisher relation is not entirely unanticipated. For instance, it should be clear that when a galaxy is a big bag of baryonic gas and has not

produced any stars (light) yet, that it can not lie on the TF relation. So, one naively expects that galaxies with high fractional gas contents should systematically be under-luminous for their line width and hence fall-off the TF relation. However, no sample to date really shows this, and attempts to look for a correlation of the residuals with gas-content (e.g. McGaugh & de Blok 1997b) have not produced anything convincing. What is unique about our data set is the appearance of galaxies with relatively large line widths that are deviating from the TF relation in this expected sense (e.g. Figure 9). In general those are the points with  $W_{20_{corr}} \geq 200 \text{ km sec}^{-1}$ . At the lower line width end, a number of studies have showed that the dispersion around the TF relation starts to increase and some galaxies are located well below the nominal relation (e.g. Matthews, van Driel, & Gallagher 1998).

In general, our sample has H I profile morphologies consistent with rotating disks (e.g. we see 2 horns). Some low line width galaxies show Gaussian or triangle profile morphologies. Inclusion of such galaxies invariably increases the scatter at the faint end because it is unclear if there is even a kinematic disk present that is rotating at some angle with respect to the line of site. So one shouldn't pay too much attention to the behavior in the TF plane for those galaxies with rotational line widths  $\leq 80 \text{ km sec}^{-1}$ .

In Figure 10 we plot the residuals from Figure 7a as a function of  $M_{HI}/L_B$ . A definitive trend toward the more H I rich objects lying the farthest off the Tully-Fisher relation is evident. This reflects a substantial reservoir of unprocessed gas and hence these potentials are under-luminous for their rotational velocity. While this is completely obvious, this is really the first sample where this effect is directly seen. This, of course, doesn't mean that there isn't a TF relation, it just means that the TF relation as defined by the luminosity versus circular velocity plane is not appropriate. If we replace luminosity by baryonic mass then there will be a large correction that is driven by the gas mass fraction. Discussion of

the existence of a "baryonic" Tully-Fisher relation, however, is beyond the scope of this paper. However, de Blok *et.al.* (1999) have undertaken a systematic investigation of the baryonic TF relation to conclude a) that such a relation exists and b) it has relatively low scatter. Under the idea of constant  $f_b$  per potential, a good baryonic TF relation must exist. Galaxies with high gas mass fraction must therefore naturally depart from the L-V relation in the sense that is finally observed in our sample.

The previous lack of detection of galaxies lying outside the  $2\sigma$  range of the H I Tully-Fisher relation in Figure 7 thus appears to be due to selection effects similar to those which created the 'Freeman law' and delayed the detection of LSB galaxies. Also akin to the original optical non-detection of LSB galaxies, these selection effects have been discussed in the literature, most notably by Briggs (1998) and Disney & Banks (1998). The H I Tully-Fisher relation, then, like the Freeman law, is a relation demonstrating our limited view of the universe, as only galaxies with similar gas mass fractions have been surveyed to date. Since gas turns into stars, the evolution in surface brightness of any disk galaxy is equivalent to evolution in decreasing gas mass fraction. The difficulty of finding high gas mass fraction galaxies is therefore equivalent to the general difficulty of detecting galaxies of extremely low surface brightness. The fact that such galaxies are now shown to exist in the nearby universe is once again a testimony to the slow evolutionary rates of some galaxies (e.g. Bothun *et.al.* 1990). Were we to have done an all sky survey at 21-cm before any optical surveys its likely that a) Freeman's Law would have never existed and b) the Tully-Fisher relation would have been harder to find. As more observations are done, and as the sensitivity of telescopes increase, we predict that most all possible regions of the H I velocity width versus magnitude plot should become populated. Indeed, one can imagine populating the upper left region simply as a result of a small starburst in one of these dormant galaxies. The sample of Salzer *et.al.* (1999) may contain such objects, but of course, such objects are **not** LSB galaxies.

## 6. Discussion

Using the refurbished Arecibo Gregorian telescope we detected 43 galaxies with  $22.0 \text{ mag arcsec}^{-2} \leq \mu_B(0) \leq 25.0 \text{ mag arcsec}^{-2}$ . The detected galaxies range in color from the very blue through the the first 21-cm detection of very red LSB galaxies, while their H I mass-to-luminosity ratios range from reasonably gas poor ( $M_{HI}/L_B = 0.1 M_\odot / L_\odot$ ) to possibly the most gas rich galaxies ever detected ( $M_{HI}/L_B = 46 M_\odot / L_\odot$ ).

Analysis of the structural properties of these galaxies show a diverse population, ranging from dwarfs to intrinsically luminous systems, though no large, Malin I-type galaxies were identified. We found no correlation between the galaxies' color and  $M_{HI}/L_B$ , confirming earlier results for HSB galaxies. We have also discovered a contingent of red LSB galaxies with  $M_{HI}/L_B > 9 M_\odot / L_\odot$ . These galaxies are generally small and if the H I distribution is similar to the optical distribution then such red galaxies are in a regime where there is no massive star formation despite having an average column density above the critical value. Either star formation is occurring without any massive star formation (e.g. the model in Table 4), or the H I distribution is very extended and we have merely detected the “optical core” of this extended gaseous distribution.

Finally, perhaps the most interesting discovery of this survey is the presence of large line width galaxies which are substantially under-luminous for their circular velocity and hence represent a significant departure from the Tully-Fisher relation. Moreover, our sample shows a clear correlation between residuals from the TF relation and gas content in the expected sense. Such a correlation exists primarily because most galaxies that form the TF relation have a very similar gas mass fraction and are in a similar evolutionary state in their history of gas-to-star conversion. Strong deviations away from this relation, such as those exhibited by our sample, indicate these LSB galaxies are not in that same state of

evolution. As much of their baryonic matter is still in the form of gas, there should be no expectation that these galaxies would fall in the same place on a luminosity vs circular velocity diagram for galaxies with lower gas content, unless the percentage of dark matter in these systems was very high. This in turn implies an unusual conspiracy - namely, the baryonic mass fraction of galaxies varies with surface brightness in such a way so as to preserve the Tully-Fisher relation. While this conspiracy can be resolved using MOND (e.g. McGaugh & de Blok 1998), it is also possible to achieve a universal baryonic mass fraction using the kind of stellar population model here, which does adequately account for the simultaneous existence of both gas-rich blue and red LSB galaxies. Under that model, we expect very red gas-rich LSB galaxies to strongly deviate from the Tully-Fisher relation in the sense observed here. The next step in unraveling all of this requires detailed investigations of the actual gas distributions in these red, gas-rich LSB galaxies.

Many thanks to Mike Davis for all his help and patience in determining the gain/temperature zenith angle corrections for the L-wide receiver. This research made use of NED, the NASA Extragalactic Database. Work on LSB galaxies at the University of Oregon is supported by NSF grant AST 9617011.

## REFERENCES

- Arp H., ApJ 1965, 142, 402
- Beauvais, C., & Bothun, G. 2000, in preparation
- Beauvais, C., & Bothun, G. 1999, preprint
- Becker, R., Mebold, U., Reif, K., Van Woerden, H. 1988 A&A 203, 21
- Bell, E., *et.al.* 1998 MNRAS 302L, 55
- Bothun, G., & McGaugh, S. 1999, in preparation
- Bothun, G., *et.al.* 1993 AJ 106, 530
- Bothun, G., Schombert, J., Impey, C., Schneider, S. 1990 ApJ 360, 427
- Bothun, G. 1990 *ASP Conference Series 10: Evolution of the Universe of Galaxies*
- Bothun, G. & Mould. J. 1987 ApJ 313, 629
- Bothun, G., Beers, T. C., Mould, J. R., Huchra, J. P. 1986 ApJ 308, 510
- Bothun, G.D., Sullivan, W. T., III, Schommer, R. A. 1982 AJ 87, 725
- Bothun, G.D. 1982 ApJS 50, 39
- Briggs, F. 1998 in *The Low Surface Brightness Universe* eds. J. Davies, M. Disney, S. Phillipps
- Broeils, A.H. 1992, Ph.D. thesis, Univ. Groningen
- Condon, *et.al.* 1998 AJ 115, 1693
- Courteau, S. & Rix, H-W. 1999 ApJ 513, 561
- Dalcanton, J., *et.al.* AJ 114, 635
- de Blok, W.J.G, *et.al.* 1999, in preparation
- de Blok, W.J.G 1997 Ph.D. Dissertation University of Groningen: Groningen
- de Blok, W.J.G., van der Hulst, J.M, McGaugh, S. 1996 BAAS 189, 8402
- de Blok, W.J.G., van der Hulst J.M., & Bothun, G. 1995 MNRAS 274, 235
- Deich, W. 1990 *ANALYZ User's Guide* Arecibo Observatory, Arecibo
- Disney, M. & Banks, 1998 in *The Low Surface Brightness Universe* eds. J. Davies, M.

Disney, S. Phillipps  
Ferguson, H. & McGaugh, S. 1995 ApJ 440, 470  
Giraud, E. 1998 AJ 116, 2177  
Hoffman, Y., Silk, J., Wyse, Rosemary F. G. 1992 ApJ 388L, 13  
Impey, C. & Bothun, G. 1997 ARA&A 35, 267  
Kennicutt, R., Jr. 1989 ApJ 344, 685  
Larson, R.B. 1986 MNRAS 218 409  
Lewis, B.M., O'Neil, K., Eder, J., & Davis, M. *The Spectral Line Manual*, in *The Arecibo User's Handbook*, C. Salter, ed. 1999  
Lewis, B.M., Helou, G., & Salpeter, E.E. 1985 ApJS 59, 161  
Marlowe *et.al.* 1999, preprint  
Matthews, L., van Driel, W., & Gallagher, J. 1998 AJ 116, 2196  
Matthews, L., & Gallagher, John S. 1997 AJ 114, 1899  
Meurer, G., *et.al.* 1996 AJ 111, 1551  
McGaugh, S. & de Blok, W.J.G. 1998 ApJ 508, 132  
McGaugh, S. & de Blok, W.J.G. 1997a ApJ 481 689  
McGaugh, S. & de Blok, W.J.G. 1997b MNRAS 290, 533  
McGaugh, S 1994 ApJ 426, 135  
Milgrom, M. 1983 ApJ 270, 365  
Mo, H. J., Mao, Shude, & White, Simon D. M 1998 MNRAS 295,319  
O'Neil, K., & Brandenburg, H. 1999, in preparation  
O'Neil, K. Verheijen, M. & McGaugh, S. 1999 preprint  
O'Neil, K. & Bothun, G. 1999 preprint  
O'Neil, K. *et.al.* AJ 1998 116, 570  
O'Neil, K. Bothun, G. & Cornell, M, 1997a, AJ 113, 1212 (OBC)  
O'Neil, K. *et.al.* 1997b AJ 114, 2448

Pickering, T. *et.al.* 1997 AJ 114, 1858  
Pierce, M. & Tully, R. 1988 ApJ 330, 579  
Quillen, A. C. & Pickering, T. E 1997 AJ 113, 2075  
Sackett, P. 1997 ApJ 483, 103  
Salzer, J. J., *et.al.* 1999, in preparation  
Salzer, J. J., *et.al.* 1993 A&AS 182, 3109  
Sandage, A., Binggeli, B. 1984 AJ 89, 919  
Schombert, J., Pildis, R., Eder, J. 1997 ApJS 111, 233  
Schombert, J., *et.al.* 1995 AJ 110, 2067  
Schombert, J., G Bothun, G., Impey, C, & Mundy, L 1990 AJ 100 1523  
Schommer, R & Bothun, G. 1983 AJ 88, 577  
Schwartzberg, J.M., *et.al.* 1995 MNRAS 275, 121  
Sprayberry, D., Impey, C. D., Bothun, G. D., Irwin, M.J. 1995a AJ 109, 558  
Sprayberry, D., Bernstein, G. M., Impey, C. D., Bothun, G. D. 1995b ApJ 438, 72  
Steinmetz, M. & Navarro, J. 1999 ApJ 513, 555  
Tinsley, B. 1972 A&A .20, 83  
Tully, R.B., & Fouque, P. 1985 ApJS 58, 67  
Tully, R.B., & Fisher, J.R. 1977 A&A 54 661  
van der Hulst, J, *et.al.* 1993 AJ 106 548  
van der Hulst, J.M., Skillman, E. D.; Kennicutt, R. C., Bothun, G. D. 1987 A&A 177, 63  
Weinberg, S. 1972 *Gravitation and Cosmology* John Wiley & Sons: New York  
White, S. *et.al.* 1993 Nature 366, 429  
Zaritsky, D., *et.al.* 1997 ApJ 478 53  
Zwaan, M., Briggs, Frank H., Sprayberry, David, Sorar, Ertu 1997 ApJ 490, 173  
Zwaan, M., van der Hulst, J., de Blok, W., & McGaugh, S. 1995 MNRAS 273, L35

---

This manuscript was prepared with the AAS L<sup>A</sup>T<sub>E</sub>X macros v4.0.

## TABLES

Table 1. The galaxy observations taken during this survey.

Table 2. The observed and derived data from this survey.

Table 3. Limiting values for the galaxy non-detections in this survey.

Table 4. The ON and OFF states of the extreme star formation model.

## FIGURES

Fig. 1.— H I profiles of all the galaxies listed in Table 2.

Fig. 2.— Two dimensional projection of all the galaxies both in our survey ( $\bullet$ ) as well as all other galaxies with published velocities and lying in the direction of the Pegasus ( $a$ ) and Cancer ( $b$ ) clusters ( $+$ ) as determined from NED. The plots show heliocentric velocity (in km/s) versus right ascension (B1950 coordinates).

Fig. 3.—  $M_B$  versus the total H I mass ( $a$ ) and the B–V color ( $b$ ) for all the galaxies in this survey ( $\bullet$ ), the LSB galaxies sample of de Blok, *et.al.* (1995, 1996) ( $+$ ), the dwarf spiral sample of Schombert, *et.al.* (1995) ( $X$ ), the late-type spiral galaxies from the Matthews, *et.al.* survey (1997) ( $\square$ ), the spiral galaxies of the Bothun, *et.al.* survey (1982) ( $\triangle$ ), and the Becker, *et.al.* (1988) survey of bright galaxies ( $\diamond$ ).

Fig. 4.— Comparisons of  $M_B$  versus central surface brightness ( $a$ ) and scale length ( $b$ ) for all the galaxies in this survey.

Fig. 5.— Total integrated H I mass ( $a$ ) and  $M_{HI}/L_B$  ( $b$ ) versus B–V for all the galaxies in detected with our survey ( $\bullet$ ), the LSB galaxies sample of de Blok, *et.al.* (1995, 1996) ( $+$ ), the dwarf spiral sample of Schombert, *et.al.* (1995) ( $X$ ), the late-type spiral galaxies from the Matthews, *et.al.* survey (1997) ( $\square$ ), the spiral galaxies of the Bothun, *et.al.* survey (1982) ( $\triangle$ ), and the Becker, *et.al.* (1988) survey of bright galaxies ( $\diamond$ ).

Fig. 6.—  $M_{HI}/L_B$  versus scale length (in kpc) for all the galaxies in detected with our survey.

Fig. 7.— Corrected ( $a$ ) and uncorrected 50% ( $b$ ) velocity widths versus absolute B magnitude for all the galaxies in detected with our survey. The solid and dashed lines are the  $1\sigma$  and  $2\sigma$  fits to the Tully-Fisher relation by Zwaan, *et.al.* (1985).

Fig. 8.—  $B-V$  versus  $B-I$  for all the galaxies detected with our survey.

Fig. 9.— Corrected 50% velocity widths versus absolute  $I$  magnitude for all the galaxies in detected with our survey ( $\bullet$ ). The solid lines are the  $1\sigma$  fits to the Virgo data of Pierce & Tully (1988) ( $+$ ), using a Virgo distance of  $20h_{75}^{-1}$  Mpc.

Fig. 10.— Residuals from fitting the galaxies detected with our survey to the Tully-Fisher relation, versus  $M_{HI}/L_B$ .



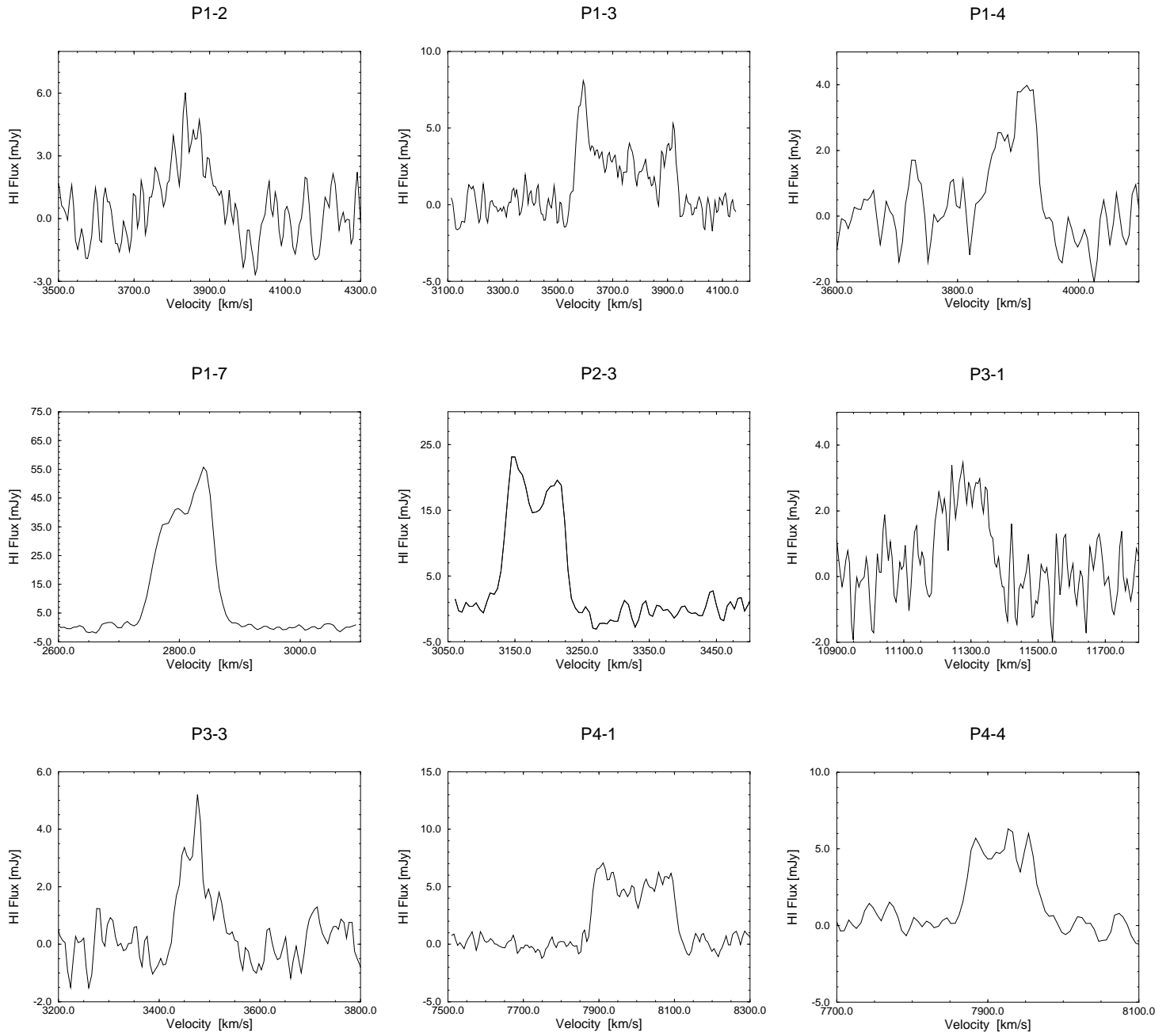


Figure 1:

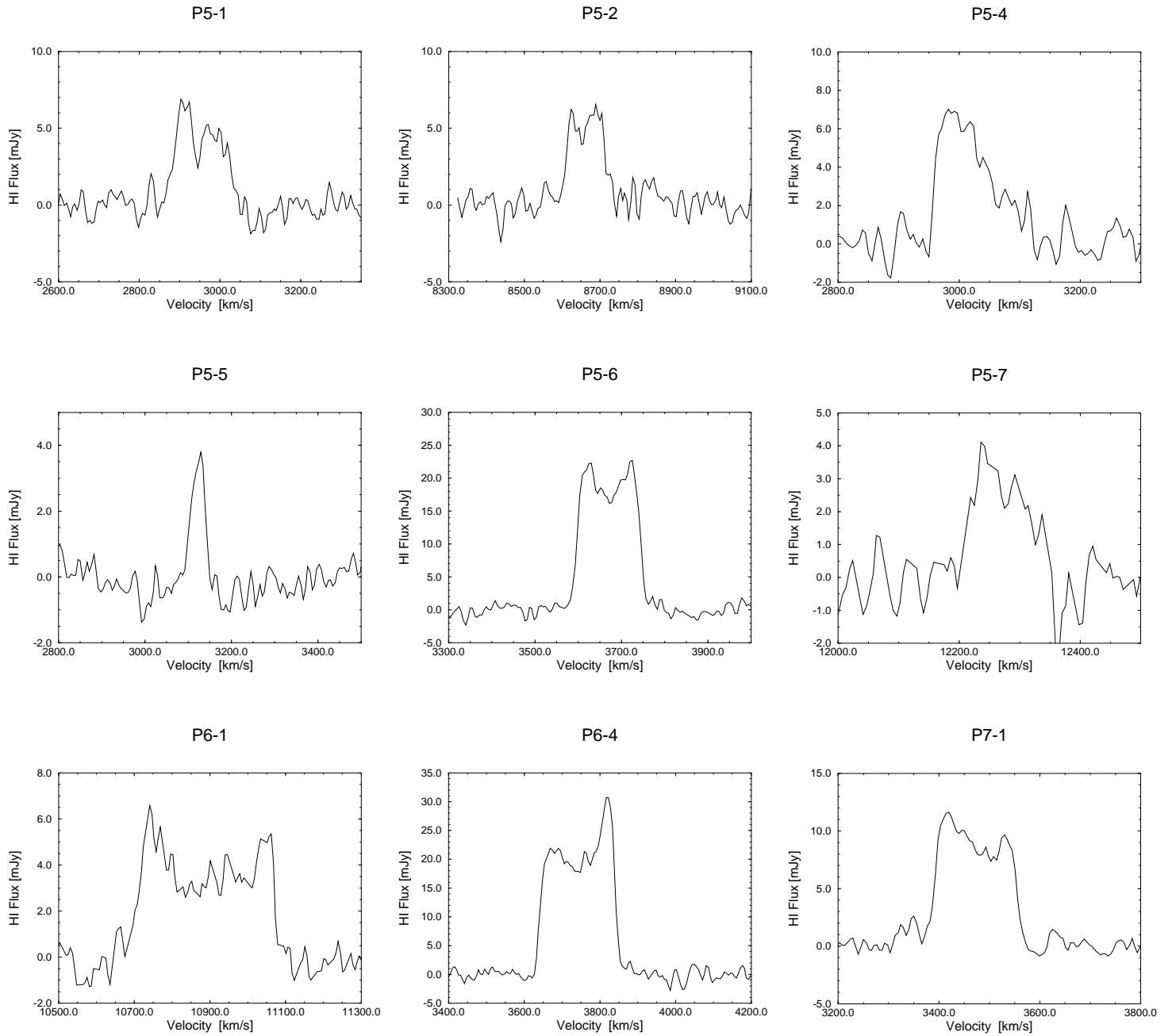


Figure 1: Continued

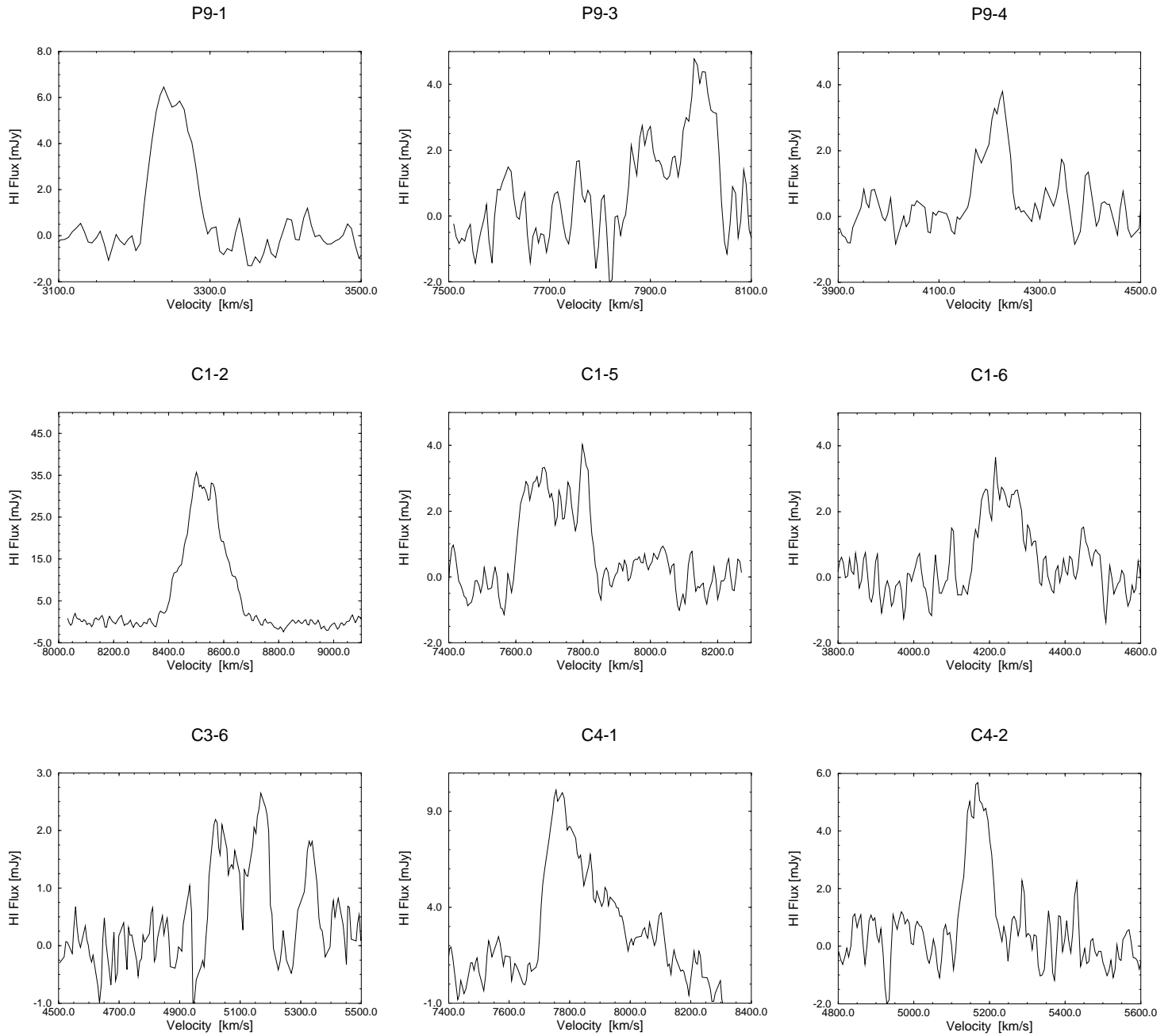


Figure 1: Continued

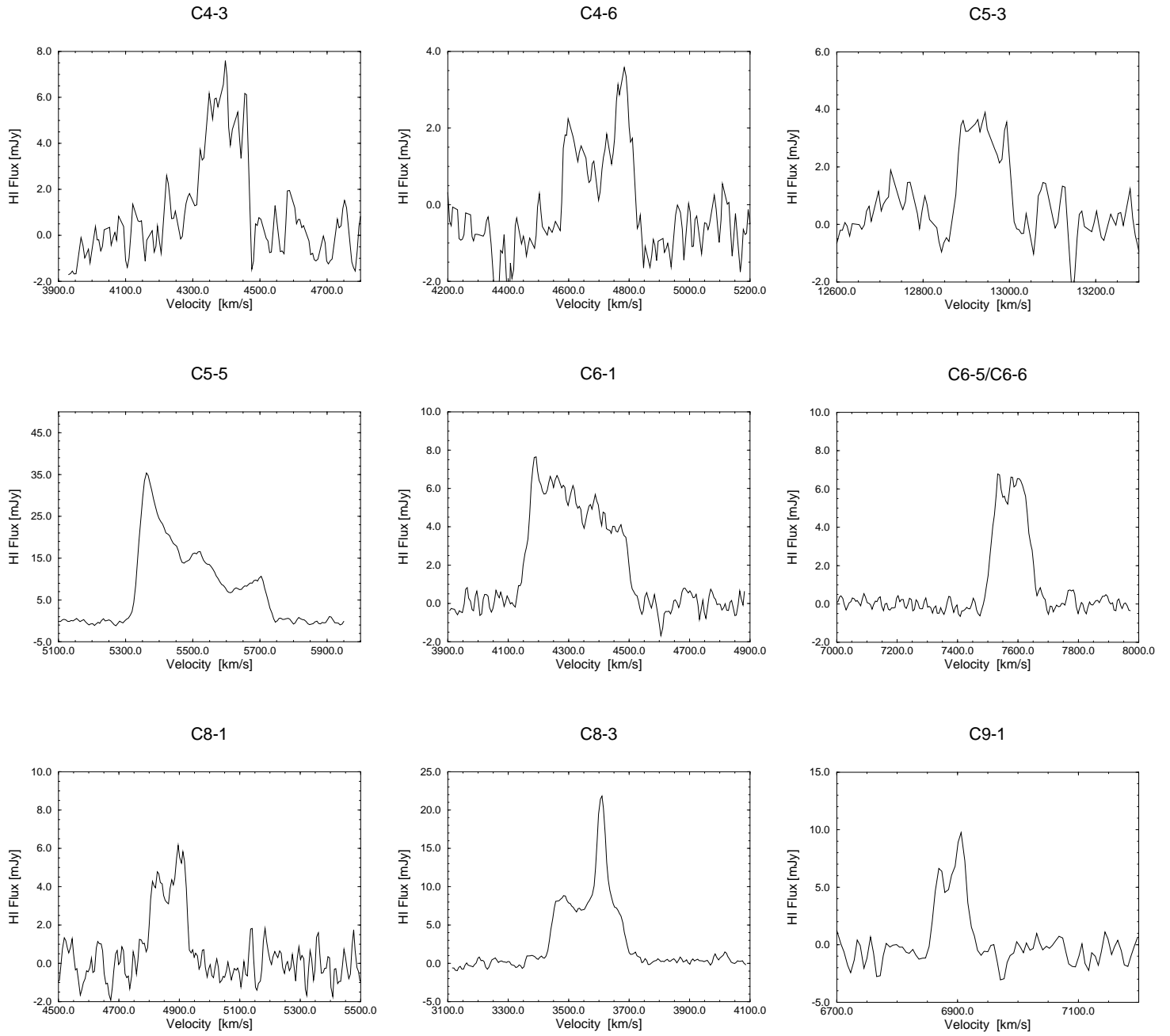
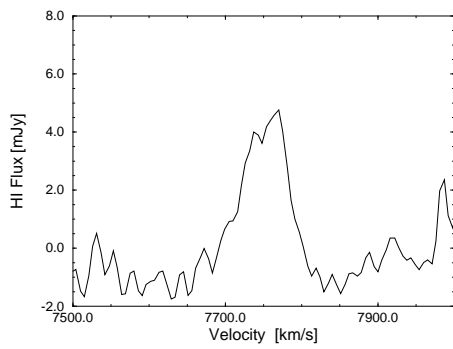
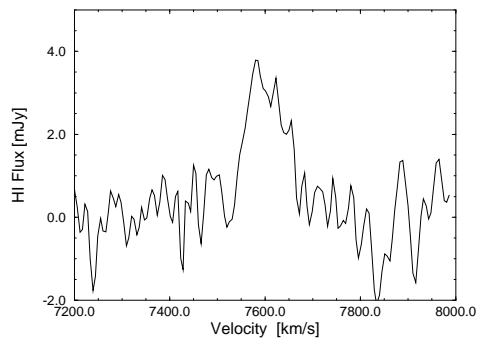


Figure 1: Continued

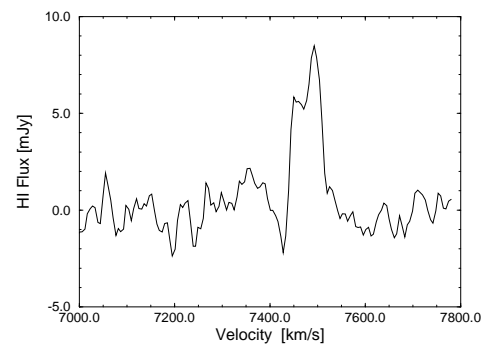
N9-2



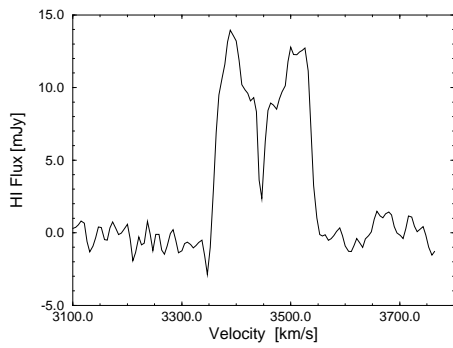
N10-3



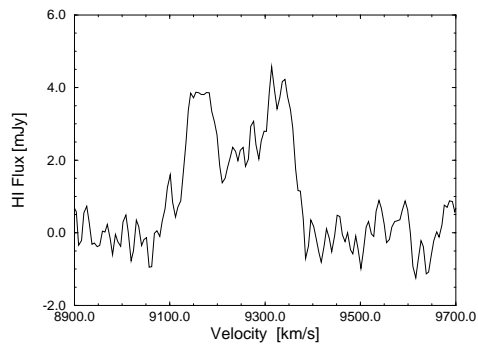
N10-4



U1-4



I1-1



I1-2

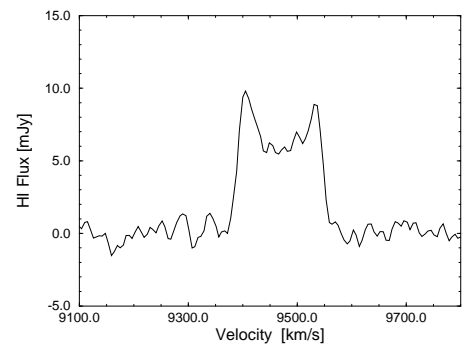


TABLE 1

Name	RA B1950	Dec B1950	L-n	L-w	Det?
P1-1	23:18:30	07:54:18	0	0	n
P1-2	23:18:44	07:48:27	1	0	y
P1-3	23:18:46	07:58:01	1	0	y
P1-4	23:19:04	07:59:01	1	0	y
P1-5	23:17:17	07:59:54	2	3	n
P1-6	23:17:23	07:39:25	1	1	n
P1-7	23:17:44	07:43:53	1	0	y
P2-3	23:14:27	07:35:55	1(2)	0	y
P2-1	23:13:44	07:36:41	1	0	n
P2-2	23:14:13	07:38:56	1	1	n
P2-4	23:14:29	08:14:57	3	3	n
P3-1	23:22:27	07:43:22	1	1	y
P3-2	23:20:31	08:01:21	1	0	n
P3-3	23:20:34	08:05:07	1	0	y
P3-4	23:20:57	08:09:54	2	1	n
P4-1	23:13:28	08:19:42	2	0	y
P4-2	23:14:48	08:23:49	1	0	n
P4-3	23:13:36	08:35:44	1	1	n
P4-4	23:13:52	08:43:50	1	0	y
P5-1	23:17:36	08:20:41	1	0	y
P5-2	23:17:11	08:24:45	1	0	y
P5-3	23:18:58	08:27:05	1	0	n
P5-4	23:18:09	08:28:38	1	0	y
P5-5	23:17:03	08:29:12	2	3	y
P5-6	23:19:15	08:45:59	2(2)	0	y
P5-7	23:16:38	08:55:20	2	2	y
P6-1	23:21:01	08:20:56	1	2	y
P6-2	23:21:06	08:35:04	1	0	n
P6-3	23:22:19	08:36:46	1	0	n
P6-4	23:20:26	08:43:01	0	1	y
P6-5	23:21:07	08:52:22	0	1	n
P6-6	23:21:35	08:57:01	1	1+1(2)	n
P7-1	23:20:27	07:23:57	2	0	y
P9-1	23:16:17	06:49:27	2	0	y
P9-3	23:15:46	06:59:29	1	0	y
P9-4	23:16:08	07:14:19	0	3	y
P10-1	23:12:54	06:48:42	3	3	n

TABLE 1

Name	RA B1950	Dec B1950	L-n	L-w	Det?
C1-1	08:17:14	20:53:51	1	1	n
C1-2	08:17:00	21:01:12	1	0	y
C1-4	08:16:29	21:09:39	4	2	n
C1-5	08:19:01	21:10:58	4	0	y
C1-6	08:16:44	21:13:41	0	2	y
C2-1	08:14:38	21:01:54	2	1	n
C3-1	08:19:59	20:56:42	1	1	n
C3-2	08:19:41	21:09:25	3(2)	1	n
C3-3	08:22:17	21:11:44	0	2	n
C3-4	08:22:06	21:36:34	0	1	n
C3-6	08:20:57	21:34:50	0	4	y
C4-1	08:21:38	21:36:50	4	2	y
C4-2	08:20:34	21:46:30	1	0	y
C4-3	08:22:30	21:50:03	0	1	y
C4-5	08:22:52	22:02:35	3	2	n
C4-6	08:21:40	22:11:00	0	2	y
C4-7	08:22:42	21:55:33	0	1	n
C4-8	08:20:05	22:07:49	2	1	n
C5-1	08:24:54	22:22:35	2	2	n
C5-2	08:24:07	22:38:37	2	1	n
C5-3	08:24:48	22:38:49	5	2	y
C5-4	08:22:43	22:56:39	0	2	n
C5-5	08:24:15	23:03:34	3	0	y
C6-1	08:24:36	21:39:59	2	0	y
C6-2	08:22:31	21:50:05	0	1	n
C6-3	08:23:45	21:55:16	0	1	n
C6-4	08:22:53	22:02:36	0	2	n
C6-5	08:24:19	22:04:12	2	0	y
C6-6	08:24:18	22:03:57	2	0	y
C8-1	08:16:09	21:44:47	0	1	y
C8-2	08:13:07	21:46:27	2	1	n
C8-3	08:14:21	21:48:32	5	0	y
C8-4	08:13:41	21:50:57	0	2	n
C8-5	08:15:18	21:58:23	1	1	n
C8-6	08:15:34	22:12:39	0	1	n
C8-8	08:14:31	22:01:40	1	1	n

TABLE 1

Name	RA B1950	Dec B1950	L-n	L-w	Det?
C9-1	08:15:16	20:21:09	2	0	y
C10-1	08:16:26	20:25:33	0	1	n
C11-1	08:20:09	20:21:08	2	2	n
C11-2	08:22:57	20:22:43	0	1	n
C11-3	08:21:13	20:32:17	3	1	n
C11-4	08:22:26	20:33:43	0	1	n
C11-5	08:19:59	20:56:41	1	1	n
N1-1	06:09:47	78:02:53	0	0	n
N1-2	06:11:05	78:28:42	0	0	n
N1-3	06:15:55	78:46:44	0	0	n
N2-1	10:40:42	24:55:13	3	0	n
N2-2	10:39:49	24:57:19	1	0	n
N2-3	10:41:23	24:58:18	2	0	n
N2-4	10:40:18	25:26:23	1+3(2)	0	n
N3-1	12:30:26	07:45:59	1	0	n
N3-2	12:31:10	08:03:32	4	0	n
N3-3	12:30:15	08:04:18	2	0	n*
N3-4	12:31:04	08:08:59	3	0	n
N7-1	14:36:31	20:23:35	0	0	n
N8-1	12:35:36	29:15:42	1	0	n
N8-2	12:34:34	29:29:34	1	0	n
N9-1	10:17:29	28:00:16	2	0	n
N9-2	10:17:33	28:23:02	0	2	y
N10-2	11:56:08	20:51:25	10	3	n
N10-3	11:54:25	21:01:52	1	0	y
N10-4	11:56:18	21:15:10	1	0	y
N10-5	11:56:17	21:27:12	5	2	n
N11-1	10:59:13	27:54:07	2	0	n
N11-2	10:59:32	28:08:49	1	0	n
U1-1	11:37:34	17:03:57	1	0	n
U1-2	11:36:56	17:08:42	2	0	n
U1-3	11:36:44	17:08:52	1+3(2)	0	n
U1-4	11:35:49	17:21:51	1	0	y
U1-6	11:37:41	17:42:17	1	0	n
U1-7	11:37:47	17:46:02	1	0	n
U1-8	11:36:47	17:07:09	2	0	n
A1-1	14:24:53	26:00:30	2+4(3)	0	n
A1-2	14:24:06	26:00:00	4	0	n
A1-3	14:23:47	26:19:44	6+3(2)	0	n
A1-4	14:24:25	26:35:30	3	0	n
A1-5	14:22:31	26:16:28	1	0	n
I1-1	15:38:32	28:31:50	3	0	y
I1-2	15:38:02	28:26:08	2	0	y

\*Possible detection

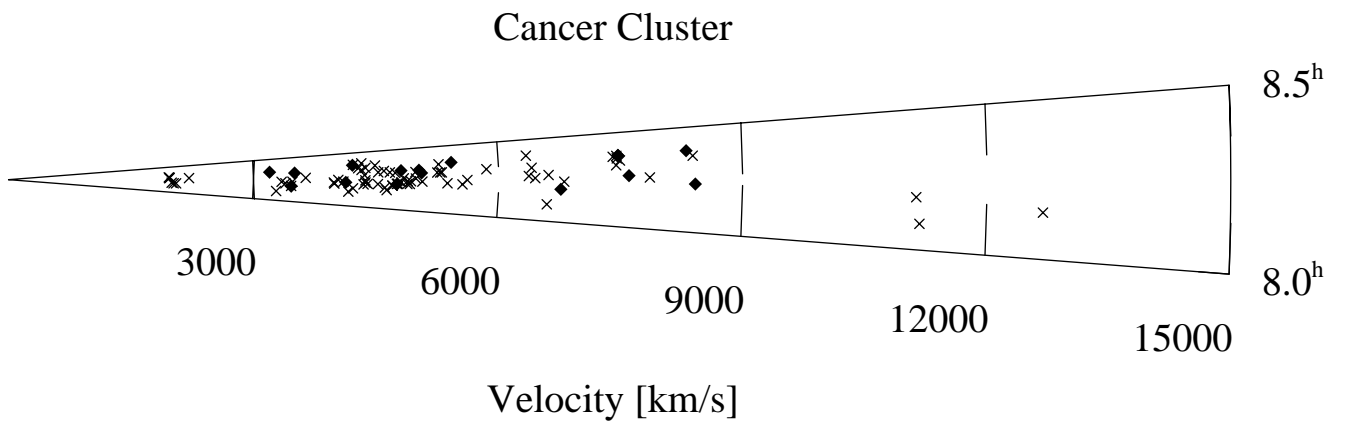
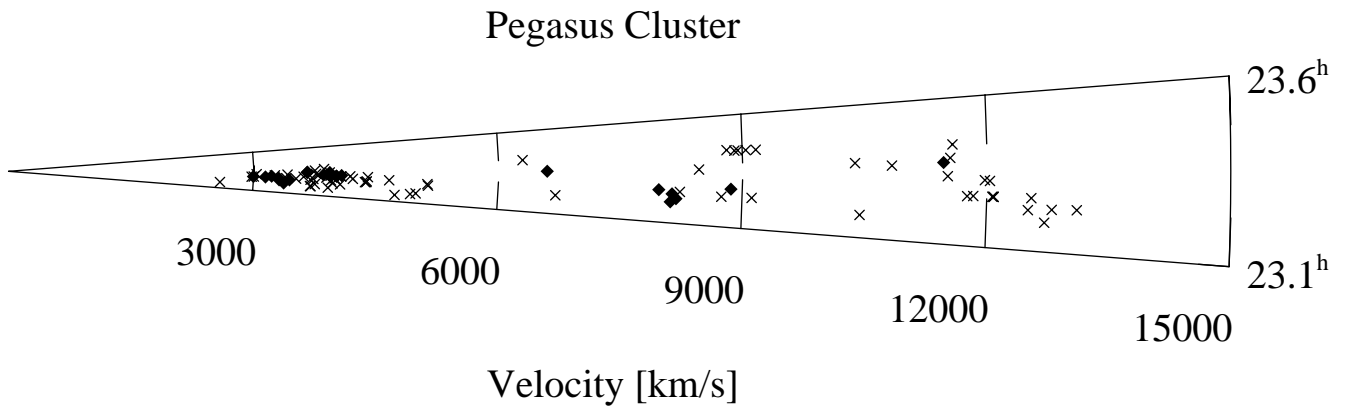
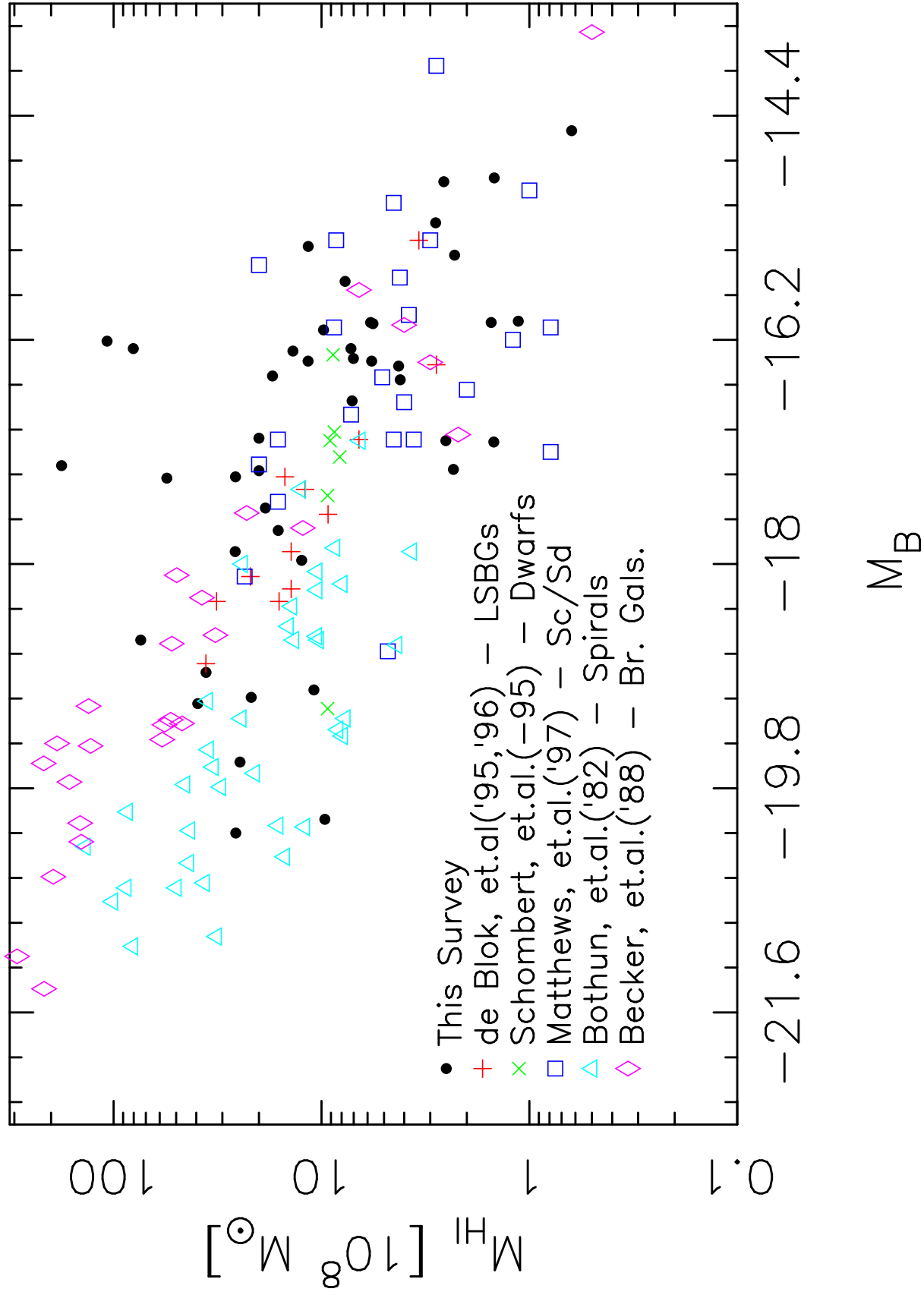


TABLE 2

Galaxy Name	Morph. Type	$v$ km/s	$B$	$M_B$	$\Delta v_{20}$ km/s	$\Delta v_{50}$ km/s	Flux Jy km/s	$M_{HI}$ $10^8 M_\odot$	$M_{HI}/L_B$ $M_\odot / L_\odot$	$M_{HI}/L_{B(\alpha)}$ $M_\odot / L_\odot$	$B-V$	$i$
P1-2	Sc	3828	18.27	-15.26	268	192(35)	0.462	2.824	2.870	1.338	0.72	62°
P1-3	Sc	3746	17.15	-16.35	391	375	1.208	7.107	2.647	2.021	0.64	39°
P1-4	Sm	3890	16.56	-17.02	104	88	0.234	1.483	0.298	0.333	0.86	34°(10°)
P1-7	Sc	2808	15.14	-17.73	135	111	4.898	16.15	1.687	1.538	0.90	30°(10°)
P2-3	Sbc	3178	17.42	-15.73	112	95	1.817	7.697	5.074	6.638	0.44	36°
P3-1	Sm	11280	16.85	-19.07	199	172	0.409	21.78	0.662	-	-	35°
P3-3	Im	3469	17.29	-16.05	108	75(35)	0.224	1.131	0.555	0.444	-	44°
P4-1	Sc	7992	16.29	-18.87	251	228	1.310	35.94	1.314	0.904	-	48°
P4-4	S:	7921	17.17	-17.97	114	99	0.474	12.45	1.043	-	-	40°(10°)
P5-1	Sm	2953	17.46	-15.52	170	149	0.626	2.289	1.831	1.244	0.48	60°
P5-2	Sm	8666	17.78	-17.55	137	113	0.593	18.63	2.297	1.274	0.68	42°
P5-4	Sc	3029	18.11	-14.93	168	129(30)	0.671	2.580	3.554	0.600	0.70	63°
P5-5	Im	3117	18.58	-14.52	71	57	0.16(0.02)	0.626	1.257	-	1.21	49°(10°)
P5-6	Sbc	3667	16.97	-16.49	367	255	3.053	17.21	5.632	0.979	0.72	72°
P5-7	Sc	12277	16.52	-19.59	148	143	0.333	24.74	0.466	-	0.73	28°
P6-1	Sd	10882	17.23	-18.61	430(35)	366	1.500	74.10	3.443	1.059	0.94	70°
P6-4	Sbc	3743	15.60	-17.90	215	201	4.433	26.02	2.325	0.892	0.67	69°
P7-1	Sc	3471	17.07	-16.27	185	164	1.429	7.218	2.894	0.747	-	75°(10°)
P9-1	Sc	3252	17.14	-16.06	84	69	0.364	1.614	0.785	1.122	-	37°
P9-3	Sm	7949	18.75	-16.37	187	177	0.439	11.60	4.242	1.281	-	55°(10°)
P9-4	Sc	4205	18.86	-14.90	91	78	0.199	1.475	2.089	3.249	-	60°(10°)

TABLE 2

Galaxy Name	Morph. Type	$v$ km/s	B	$M_B$	$\Delta v_{20}$ km/s	$\Delta v_{50}$ km/s	Flux Jy km/s	$M_{HI}$ $10^8 M_\odot$	$M_{HI}/L_B$ $M_\odot / L_\odot$	$M_{HI}/L_{B(\alpha)}$ $M_\odot / L_\odot$	B-V	$i$
C1-2	Sc	8531	18.10	-17.21	268	201(50)	5.846	178.0	30.03	28.41	1.12	28°
C1-5	Sc	7717	16.08	-19.01	240	229	0.436	10.87	0.321	0.346	0.73	67°
C1-6	Sc	4240	16.77	-17.01	173	145	0.336	2.524	0.512	-	0.88	50°
C3-6	Sbc	4010	16.41	-17.24	218	189	0.344	2.321	0.381	0.160	0.52	68°
C4-1	Im	7905	17.83	-17.31	419	410	2.118	55.43	8.527	-	0.57	32
C4-2	Im	5168	17.69	-16.52	103	85	0.374	4.184	1.329	-	1.28	67°(10°)
C4-3	Sm	4390	17.48	-16.37	170	151	0.711	5.738	2.100	1.042	0.49	55°
C4-6	Sc	4703	-	-	263	241	0.714	6.610	-	-	-	-
C5-3	Im	12942	18.88	-17.30	130	123	0.370	25.94	4.027	2.449	1.18	51°(10°)
C5-5	S:	5524	18.08	-16.27	402	392	6.286	80.44	32.25	5.922	0.97	70°(10°)
C6-1	Sc	4322	17.53	-16.29	385	333	1.755	13.72	5.399	3.841	-	47°
C6-5†	Sc	7579	17.80	-17.25	170	143	0.830	19.99	3.248	-	-	62°
C6-6†	Sc	7579	18.06	-16.99	170	143	0.830	19.99	4.128	5.102	-	54°
C8-1	Sc	4865	18.02	-16.06	144	127	0.585	5.803	2.822	1.717	0.58	59°(10°)
C8-3	Sm	3570	17.69	-15.72	263	256	2.262	12.07	8.057	16.01	0.55	61°(10°)
C9-1	Sm	6884	18.15	-16.69	64	54	0.359	7.123	1.940	1.270	0.90	52°(10°)
N9-2	Im	7746	18.89	-16.21	118	89	4.282	107.6	45.63	36.59	0.82	47°
N10-3	Im	7626	18.99	-16.07	155	137	0.232	5.652	2.724	1.851	0.88	48°
N10-4	Sc	7478	18.90	-16.12	80	73	0.418	9.778	4.502	2.520	0.37	35°
U1-4	Sc	3450	13.08	-20.05	191	181	1.932	9.632	0.0988	0.296	-	55°
I1-1	Sc	9237	14.82	-20.16	298	262	0.723	25.83	0.288	0.196	0.78	77°
I1-2	Sc	9469	16.42	-19.12	175	162	1.048	39.39	1.144	0.771	0.71	44°



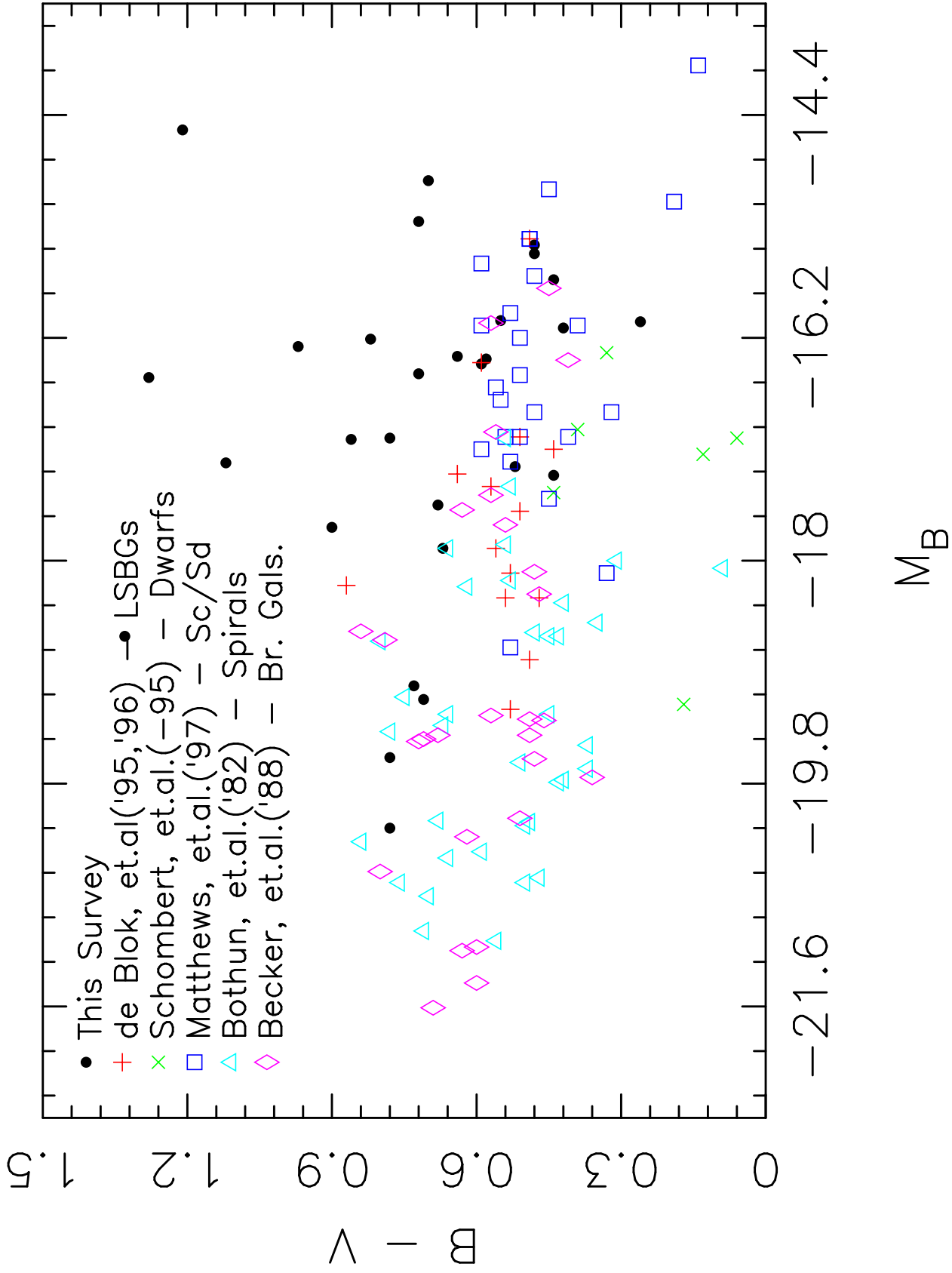
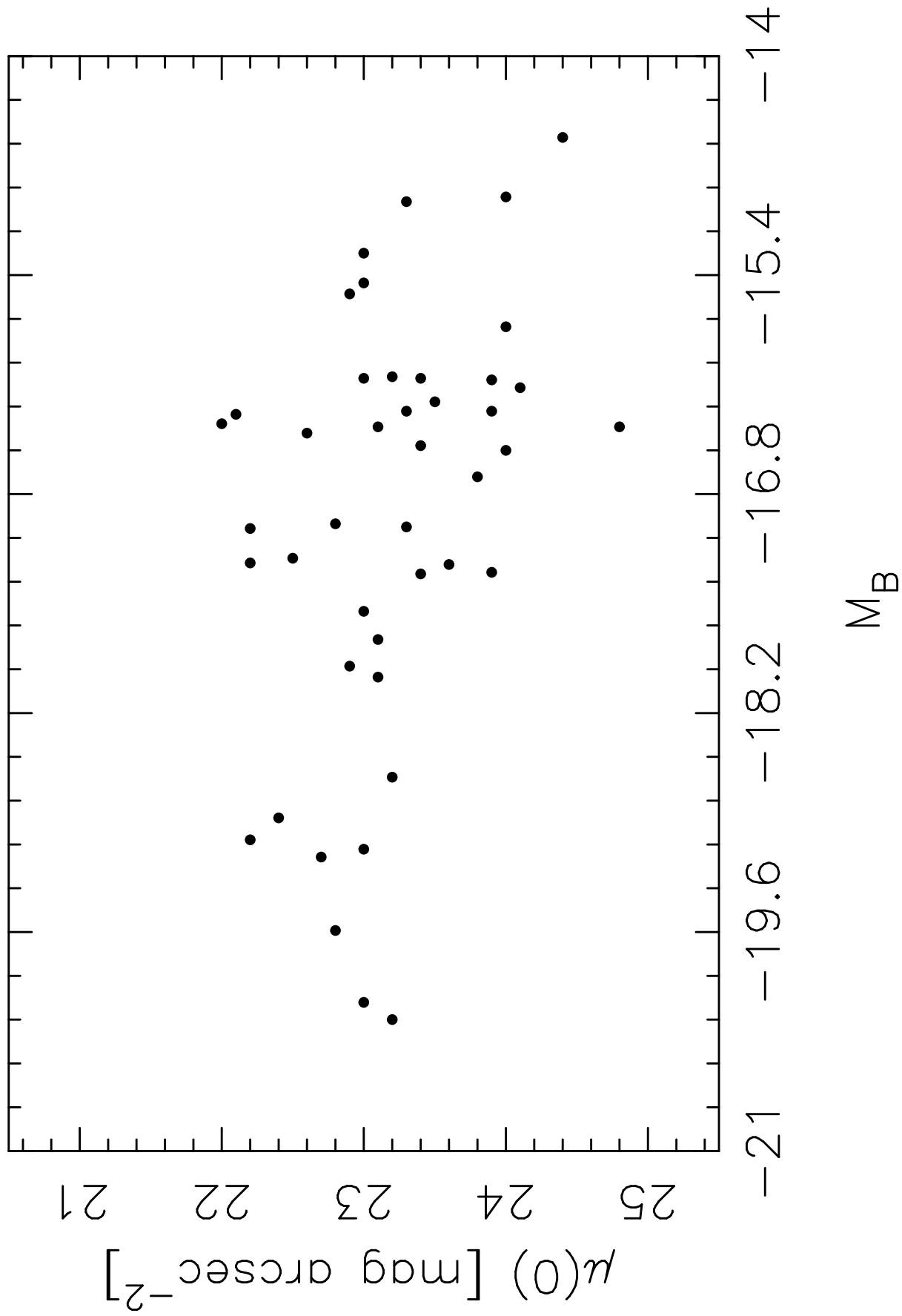


TABLE 3

Name	$1\sigma$ Detection (mJy)	
	L-Narrow	L-Wide
P1-5	1.0	0.5
P1-6	1.4	1.7
P2-1	1.4	-
P2-2	1.4	1.3
P2-4	0.7	1.0
P3-2	1.4	-
P3-5	0.9	1.2
P4-2	1.4	-
P4-3	1.5	1.5
P5-3	1.4	-
P6-2	1.3	-
P6-3	1.2	-
P6-5	-	1.3
P6-6	1.6	1.4
P10-1	0.8	0.9
C1-1	1.5	1.4
C1-4	0.8	1.0
C2-1	1.0	1.4
C3-1	1.2	1.1
C3-2	1.4	1.2
C3-3	-	1.1
C3-4	-	2.4
C4-5	1.3	1.4
C4-7	-	1.4
C4-8	0.8	2.1
C5-1	1.5	4.6
C5-2	1.0	1.2
C5-4	-	2.6
C6-2	-	2.6
C6-3	-	1.6
C6-4	-	1.3
C8-2	0.9	1.4
C8-4	-	1.4
C8-5	1.4	1.4
C8-6	-	1.5
C8-8	1.4	2.0
C10-1	-	1.4
C11-1	0.9	1.3
C11-2	-	1.5
C11-3	0.9	1.7
C11-4	-	1.5
C11-5	1.4	3.8
N2-1	0.7	-
N2-2	1.5	-
N2-3	1.4	-
N2-4	2.7	-
N3-1	1.9	-
N3-2	1.9	-

TABLE 3—*Continued*

Name	$1\sigma$ Detection (mJy)	
	L-Narrow	L-Wide
N3-3	1.9	-
N3-4	1.0	-
N8-1	1.3	-
N8-2	1.4	-
N10-2	0.5	1.0
N10-5	0.8	1.0
N11-2	2.4	-
U1-1	2.4	-
U1-2	2.4	-
U1-3	2.5	-
U1-6	1.5	-
U1-7	1.4	-
U1-8	2.5	-
A1-1	2.0	-
A1-2	0.4	-
A1-3	0.5	-
A1-4	0.9	-
A1-5	1.0	-



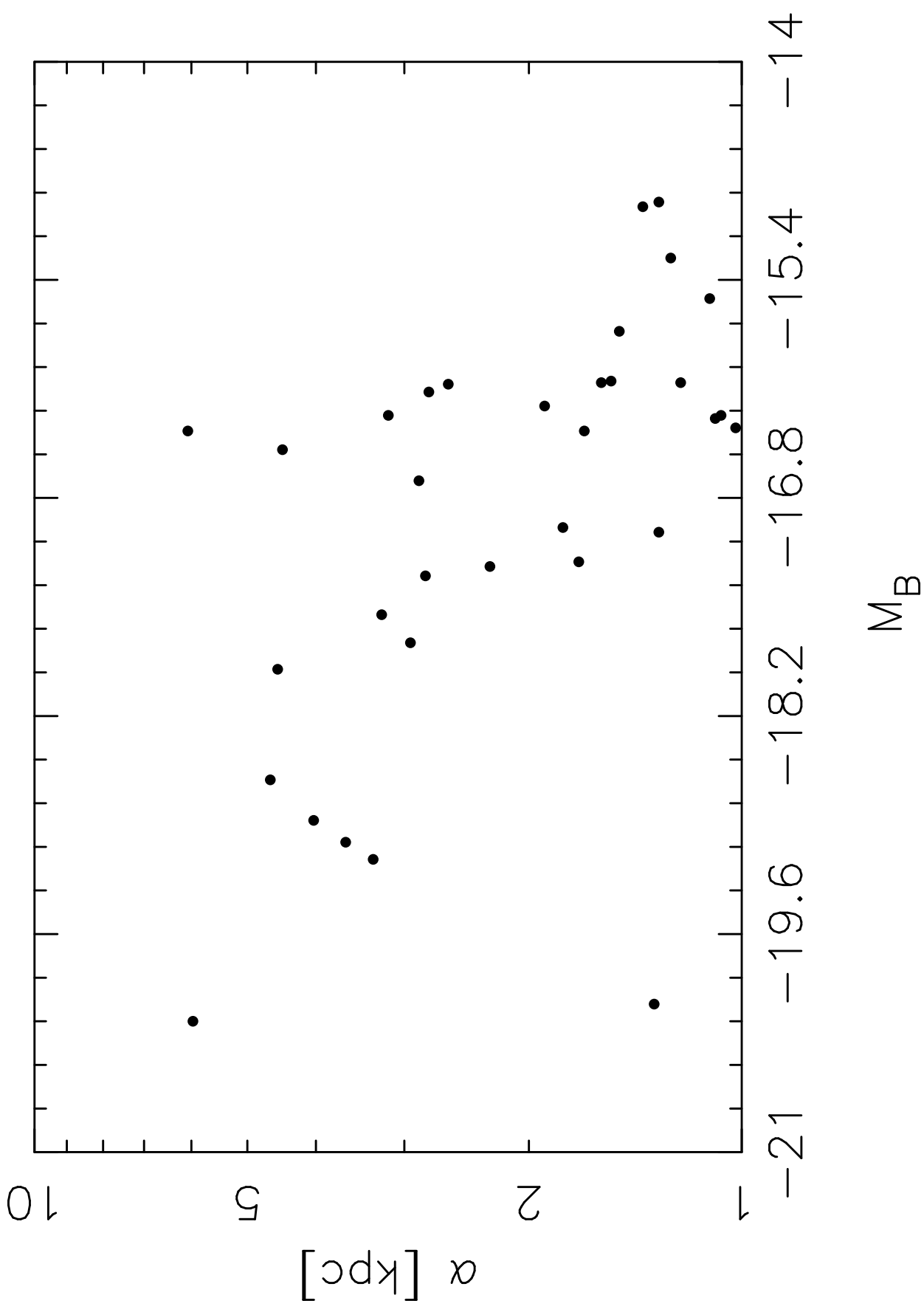


TABLE 4

	OFF State	ON State
Model 1:		
$L_B$	$1.0 \times 10^9$	$3.2 \times 10^9$
$B - V$	0.88	0.38
$M/L_B$	30.	9.4
Giant Br. Contr.	9.0%	3.0%
AFO Star. Contr.	0.0%	68%
Model 2:		
$L_B$	$1.0 \times 10^9$	$3.6 \times 10^9$
$B - V$	1.02	0.42
$M/L_B$	34.	9.5
Giant Br. Contr.	4.0%	1.0%
AFO Star. Contr.	0.0%	72%
Model 3:		
$L_B$	$1.0 \times 10^9$	$4.4 \times 10^9$
$B - V$	1.02	0.33
$M/L_B$	34.	7.9
Giant Br. Contr.	4.0%	1.0%
AFO Star. Contr.	0.0%	77%
Giant Branch and AFO star contributions are calculated in the B band.		
Models 1 and 2 use MS: A0,F0,G2,G5,K0,M0,M5; Giant: K3 type stars.		
No stars more massive than $2.0M_\odot$ ever form in models 1 and 2.		
Model 3 includes Stars of type O6		

